Bachelor thesis

Submitted in the fulfillment of the requirements for the degree of 'Bachelor of Science (B.Sc.) Physics'to the faculty of Science at the University of Potsdam

Extinction and reddening of hot subdwarfs from the Gaia catalogue

Submitted to:

Prof. Dr. Dr. Stephan Geier

Chair of stellar astrophysics

University of Potsdam

by:

Niklas Polei

Zum Mühlenteich 4

14476 Potsdam

Matricle number: 785826

Potsdam, October 23, 2019

Contents

1 Abstract

Hot subdwarf stars are in the late stages of stellar evolution. They finished core-hydrogen burning and then evolved via different possible evolution scenarios to core helium-burning objects with only a thin atmosphere left.

There are not many known hot subdwarfs. Their formation and the properties of the hot subdwarf population are not well understood either. A key to understanding hot subdwarfs are their photometric properties. These are altered by the interstellar medium which consists of gas and dust which causes reddening and extinction of the light. This work tries to account for these effects and tries to correct for them.

I used a dust map and Gaia or APASS data to calculate extinction and reddening corrected values for the absolute magnitude and color index values of the hot subdwarf candidates in the limits of the dust map. I also verified the differences between the use of Gaia and APASS apparent magnitude data.

The correction for reddening shows that for all three methods (Gaia magnitudes and distances, Gaia magnitudes and 5 pc per cube, Gaia distances and APASS magnitudes) the correction does not work for all the stars because they have too blue colors after the correction. The amount of these stars varies strongly from method to method. The rest of the stars satisfies the other criteria for the use of Gaia magnitudes but when using APASS magnitudes this is not the case. Some stars do not satisfy the hot subdwarf criteria in this method.

The stars are, because of some selection effects, oddly distributed on the sky. Also the extinction is distributed oddly. This leads to some unexpected results when looking at which stars, distance- and positionwise, are satisfying the hot subdwarf criteria and which stars are not.

The results differ using Gaia and APASS magnitudes, which has an impact on which stars are excluded and their nature. Also the fractions of excluded stars partly show differences using the differnt methods.

2 Hot subdwarfs

Hot subdwarfs are core-helium burning objects with just a small non-burning hydrogen layer. They are therefore very hot ($T_{\mathrm{eff}} > 20000$ K for sdB and $T_{\mathrm{eff}} > 40000$ K for sdO stars) but not as luminous as the main sequence O and B stars. This positions the hot subdwarfs in Figure 1 on the Extreme Horizontal Branch (EHB) between the main sequence and the white dwarf sequence in the Hertzsprung-Russell-diagram (Heber 1986).
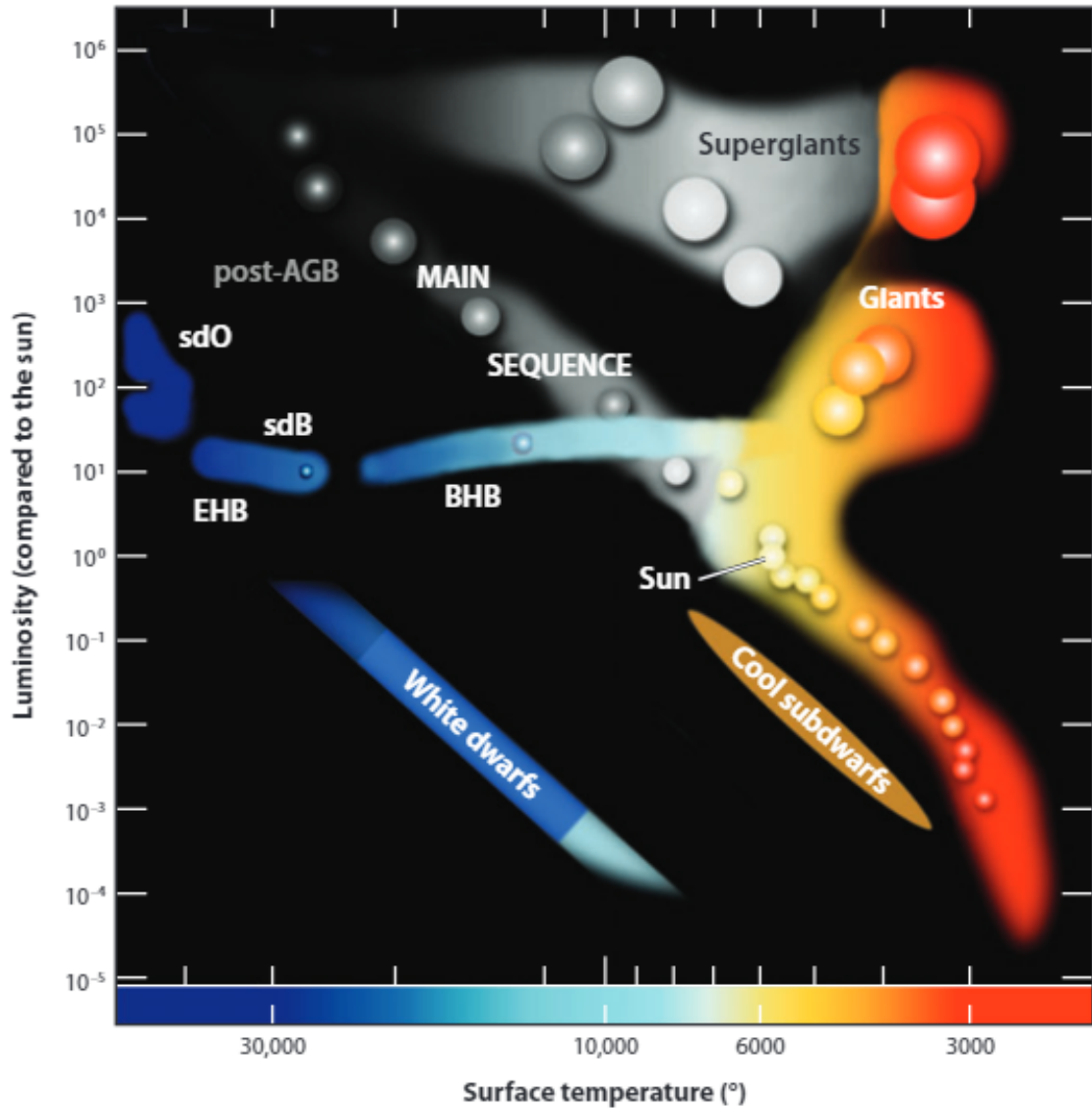
Figure 1: Hertzsprung-Russel-diagram (Heber 2009)

The chemical composition of hot subdwarfs can be very different between the two classes sdO and sdB and within those classes as well. The main difference between sdBs and sdOs is that sdOs show HeII lines due to their higher temperatures and sdBs don't (Moehler et al. 1990). In both classes stars exist, which have a helium rich atmosphere, then dubbed He-sdO or He-sdB. There are also a few stars which show an overabundance of heavy elements such as elements of the iron group (Blanchette et al. 2008). These different atmospheric compositions are caused by diffusion and/or mixing of the atmosphere (Cassisi et al. 2003).

Hot subdwarfs can be found in binaries and as single stars either in the disk, the bulge, the halo or globular clusters (Kawka et al 2015; Busso et al. 2006; Geier et al. 2017). So they can be found everywhere in the Galaxy. They can also be Population I or Population II stars, although the determination of the population membership is difficult because atmospheric diffusion leads to over- or underabundances of elements with respect to their

2

primordial compositions (Heber 2016).

Hot subdwarfs in binaries can have different companions. Those can be other hot subdwarfs, white dwarfs, low-mass main sequence stars (Copperwheat et al. 2011; Vos et al. 2013) and brown dwarfs (Geier et al. 2011). The companion type can be determined from the spectrum either directly by identifying it's spectral lines or indirectly from the variation of the spectral lines due to Doppler reflex motion of the hot subdwarf. When only the hot subdwarf can be seen it can be difficult to determine the companion type because only the radial velocity variation can be observed and the inclination of the system is not known. Some candidates for a hot subdwarf binary with a neutron star or black hole companion have been proposed as well (Geier et al. 2010b).

There are some other unique hot subdwarfs which are interesting. For example the sdO US 708 which is unbound to the galaxy because of it's high velocity ($v = 1082 \frac{\mathrm{km}}{\mathrm{s}}$) (Brown et al. 2015).

Hot subdwarf binaries with white dwarf companions of sufficiently high masses are candidates for Supernova Ia progenitors (Maxted et al. 2000). Also hypervelocity single hot subdwarfs are thought to be the result of Supernova Ia explosions. So far only one such system is known (Kupfer et al. 2015).

There are several hot subdwarfs in binaries which host circumbinary planets discovered by eclipse-time variations. These planets could have survived the subdwarf formation or formed after the subdwarf formation from the remnants of the envelope (Lee et al. 2009).

3 Formation scenarios

As soon as stars start core-helium burning after the red giant phase they move onto the horizontal branch. The core mass is constant at this stage and only the envelope mass differs from star to star (Han et al. 2003). Those stars which lose almost their entire envelope end up at the blue end of the horizontal branch and ultimately become hot subdwarfs. Subsequently they evolve towards higher temperatures in the Hertzsprung-Russell-diagram and reach the white dwarf cooling track (Heber 2016). The process of how the star loses nearly it's entire envelope is not yet known, but there are some scenarios proposed.

3.1 Hot flasher

Normally, low mass stars experience the helium flash at the tip of the red giant branch. However, after sufficient mass loss on the red giant branch the stars won't experience the helium flash at the tip of the red giant branch, but will first evolve towards the white dwarf cooling track. The helium flash will then occur on the white dwarf cooling track. If the helium flash occurs late after reaching the white dwarf cooling track, mixing will take place and enrich the atmosphere with helium and also sometimes carbon or nitrogen

(Lanz et al. 2004; confirmed by simulations: Miller-Bertolami et al. 2009).

3.2 Binary evolution

3.2.1 Common envelope

One of the stars in a binary system evolves into a red giant first. If the companion is close enough it will be engulfed by the envelope of the red giant. Through friction with the envelope the orbit shrinks and the envelope is removed. The result is a close hot subdwarf binary with a small companion star (Paczynski 1976). If the small companion is a main sequence star a second common envelope phase may occur.

3.2.2 Roche lobe overflow

In this scenario the companion will strip the whole envelope of the red giant through Roche lobe overflow. This happens in long period binaries and the result is a hot subdwarf with a main sequence star (Chen et al. 2013). A second Roche lobe overflow won't happen in this type of binary but a common envelope phase can occur if the main sequence star becomes a red giant. Then the result is again a very close binary.

3.2.3 White dwarf merger

In this formation scenario a close binary of two helium white dwarfs shrinks due to the radiation of gravitational waves and finally merges. If the combined mass is lower than the Chandrasekhar mass a helium rich single hot subdwarf will form (Webbink 1984).

4 Volume-limited hot subdwarf catalogs

Currently, there are three major hot subdwarf catalogs in the literature. The oldest one is a spectroscopically selected catalog. For this catalog the hot subdwarfs were selected by spectroscopic criteria from the literature. The 2300 listed stars are confirmed hot subdwarfs (Østensen 2006).

Before the release of Gaia DR1 a new hot subdwarf catalog was compiled. It includes data from several recent surveys such as Kepler, MUCHFUSS or SDSS. It also contains the stars from the before mentioned spectroscopic catalog. In total there are 5613 spectroscopically classified stars in the catalog. Since Gaia data were not yet included, this catalog is by far not complete (Geier et al. 2017).

The most recent catalog consists of all hot subdwarfs, both confirmed and candidates, identified with Gaia data. It consists of 39800 stars and uses Gaia colours, distances and proper motions. It was compiled using selection criteria derived from the properties of the already confirmed hot subdwarfs (Geier et al. 2019).

There are several selection effects which affect those catalogs. For example magnitude limited samples, such as the Gaia sample, which only include stars up to a certain apparent magnitude could exclude stars which are nearer than other stars, but fainter. Also there can be selection effects in regions with high extinction because stars are strongly reddened and therefore assigned a wrong stellar type.

In the case of hot subdwarfs, where no all-sky survey was conducted, there can be selection effects due to the non-uniform sky coverage. Most hot subdwarfs have been discovered as blue stars at high Galactic latitudes.

In contrast to that a volume-limited sample, which is complete or nearly complete in a certain volume around the Sun should be unbiased. In this volume all stars of a certain type, for example hot subdwarfs, are known.

With such a volume-limited sample of hot subdwarfs it would be possible to answer some fundamental questions related to hot subdwarf formation and evolution.

It is not clear how subdwarfs form. There are the aforementioned formation scenarios, but whether only one of those or a combination of several or all of them are valid, is still unknown. In a volume-limited sample the number of hot subdwarf stars in certain configurations, such as close or wide binaries or single stars, can be counted and by comparison to the number of progenitor systems, possible formation channels could be confirmed or ruled out.

The population of hot subdwarfs itself can be charaterised better with a volume-limited sample. The exact ratio of sdOs to sdBs or helium-enriched to helium-depleted stars is not known. With this information it could be checked if sdO stars really evolve from sdBs. If this is the case there have to be stars in a transition phase. The exact ratio of sdBs to sdOs would reveal if this evolution is plausible.

Therefore it is important to compile a complete volume-limited sample of hot subdwarfs. To select a volume-limited sample reddening and extinction have to be taken into account because especially in the Galactic plane there is gas and dust affecting the light coming from the stars. For hot subdwarfs this has not been done before.

5 Interstellar reddening and extinction

5.1 Composition of the interstellar medium

The interstellar medium consists of many gas and dust clouds with different compositions. The most common clouds are hydrogen clouds which consist of mostly neutral molecular hydrogen (Woodall et al. 2007). Around young hot stars in star forming regions there are HII regions consisting of ionized hydrogen (catalogue of HII regions: Anderson et al. 2014) and around dead stars there can be planetary nebulae consisting of the expelled ionized envelope of the star where products of stellar nucleosynthesis can be observed di-

rectly (Kwitter et al. 2014). Such clouds are then called emission nebulae as for example the Orion nebula in the star forming region of Orion (Palla&Stahler 1999) or the Ring nebula, a planetary nebula around a white dwarf (van Hoof et al. 2010). Other interstellar clouds form through supernovae and contain many heavy elements even above iron (Chevalier 1974).

Interstellar dust consists of grains of macroscopic size. These grains are mostly made of silicates or carbonaceous material (Millar 2015). Chemical compounds with the dust grains make it possible for atoms and molecules to attach to the dust grains. The surfaces of dust grains also allow molecules to form (Hasegawa et al. 1992). There is a huge variety of molecules in the interstellar medium, many of them with hydrogen as a component (McElroy et al. 2013).

5.2 Diffuse interstellar bands

Diffuse interstellar bands are absorption bands best observed in spectra of hot stars. They can have widths of several Ångstrom but are shallow (Hobbs et al. 2009). Still they alter the spectra of stars. The carriers of diffuse interstellar bands are not known except for the fulleren C_{60} which is a confirmed carrier (Walker et al. 2015). Other fullerenes and polycyclic aromatic hydrocarbons are suggested as other carriers (Salama et al. 2011). Diffuse interstellar bands also have their origin in the interstellar medium.

5.3 Reddening

The interstellar medium preferentially absorbs shorter wavelengths. This has it's origin in the dust grain size distribution (Fitzpatrick 2004). Because there are dust grains with a size up to a few microns, the light with wavelengths smaller than a dust grain can be absorbed and scattered. Wavelengths larger than a dust grain are not affected by that grain. This effect is strongly wavelength dependent and follows different laws in the different wavelength ranges of the electromagnetic spectrum. In Figure 2 there is a distinct bump with higher absorption at around 2175Å (Fitzpatrick 1999) of which the origin is not clear, but it is suggested that it comes from graphite.

The result of this is that the light of a star that reaches us is redder than when it was emitted. To account for this the color excess is defined:

$$E_{B-V} = (B-V)_{\text{observed}} - (B-V)_{\text{emitted}} \tag{1}$$

where B is the apparent magnitude in the B-band and V the apparent magnitude in the V-band. With the observed apparent magnitude and the extinction, explained in the next part, the emitted $B-V$ can be determined.
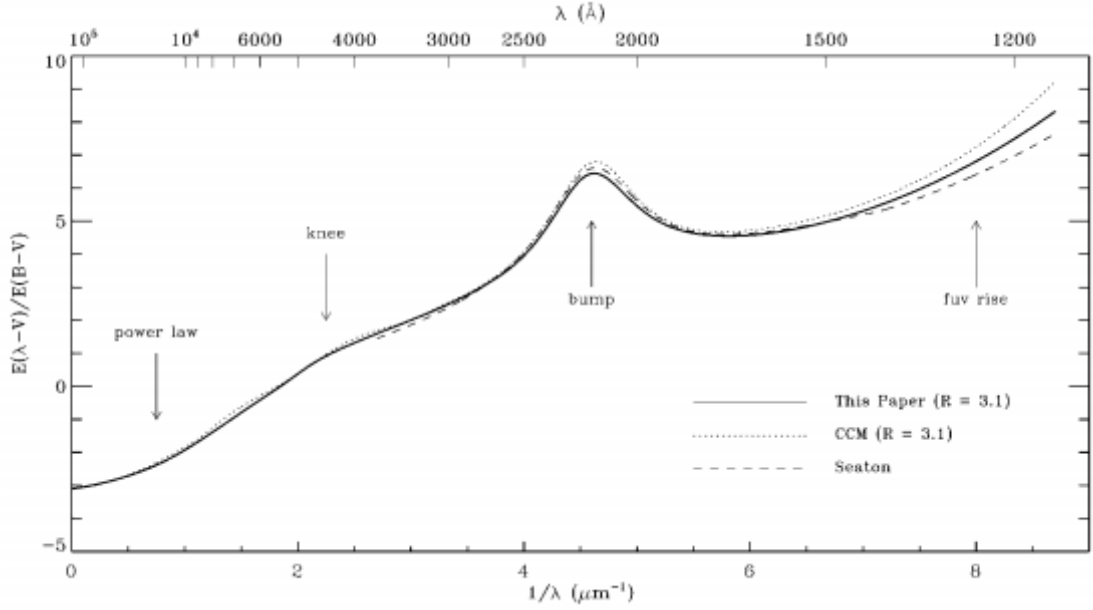
Figure 2: Interstellar extinction curve (Fitzpatrick 1999

5.4 Extinction

Extinction takes into account the absorption at all wavelengths. If the extinction to an object is known the apparent magnitude can be corrected. There is a relation between color excess and extinction which is more or less constant in the Milky Way:

$$\frac{A_V}{E_{B-V}} = 3.1 \tag{2}$$

where A_V is the extinction in the V-band.

6 Data

6.1 Hot subdwarf catalog

The data used for the hot subdwarfs is taken from the hot subdwarf catalog compiled by Geier et al. (2019). It is based on data from the Gaia mission which can measure distances and positions as accurate as never before. It contains 39800 stars which were selected by the following criteria that were established by Geier et al. (2019):

- the color excess of the RP and BP passbands of Gaia should satisfy $G_{BP} - G_{RP} < 0.7$ mag

- the absolute magnitude should be $-1.0 < M_G < 7.0$ mag

- to exclude main sequence stars empirical colour-criteria derived from known hot subdwarfs should be satisfied:

7

- for stars with $-1.0 < M_G \leq 1.0$: $M_G \geq 11.76 \cdot (G_{BP} - G_{RP}) + 2.53$

- for stars with $1.0 < M_G \leq 3.8$: $M_G \geq 5.6 \cdot (G_{BP} - G_{RP}) + 1.84$

- for stars with $3.8 < M_G \leq 7.0$: $M_G \geq 16 \cdot (G_{BP} - G_{RP}) - 1.8$

For larger distances the stars were also selected by reduced proper motions. With this method hot subdwarfs and white dwarfs can be distinguished.

The catalog is available at `http://vizier.u-strasbg.fr/viz-bin/VizieR?-source=J/A+A/621/A38&-to=3` and I retrieved it on 21st June 2019.
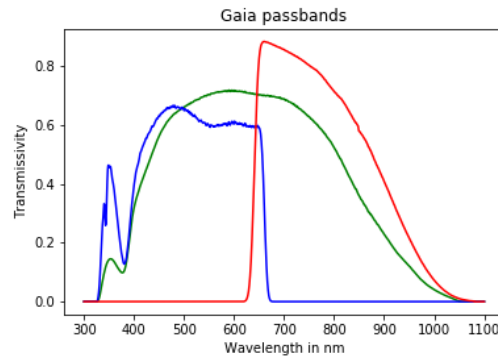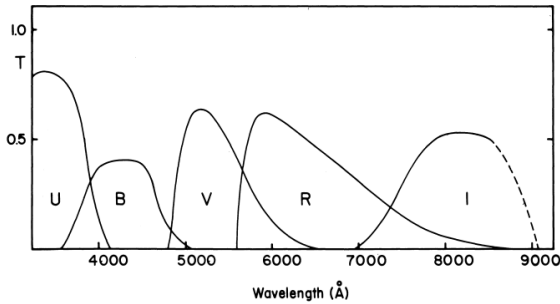
6.2 Passbands

Figure 3: UBVRI system (Graham 1994)   Figure 4: Gaia filter system (Evans 2018)

Above the Johnson UBVRI (Figure 3) and the Gaia filter system (Figure 4) are shown. The APASS survey uses the Johnson UBVRI filter system which is also used to give the reddening in the dust map. The APASS survey contains photometric data of stars, covering the whole sky.

The G band of the Gaia filter system (green in Figure 4) covers the whole visible wavelength range. The BP (blue in Figure 4) and RP (red in Figure 4) bands cover the short and long wavelength half of the visible wavelength range respectively, meaning BP covering $325\,\text{nm} - 670\,\text{nm}$ and RP covering $640\,\text{nm} - 1080\,\text{nm}$. In contrary the B and V band in the Johnson system cover just a small range of wavelength, B covering $350\,\text{nm} - 500\,\text{nm}$ and V covering $480\,\text{nm} - 650\,\text{nm}$. The Gaia filters cover much more of the red end, even into the infrared, of the wavelength spectrum. This influences the color excess and extinction. Tis systematic effect will be studied later.

6.3 Dust map

The dust map used in this work is computed by Capitanio et al. (2017). They used several thousand target stars and diffuse interstellar bands to compute the extinction. They used distances from several missions dedicated for distance measurement such as Gaia or Hipparcos. The extinction is then computed using the Bayesian inversion where the

analytical solution of the opacity distribution is optimized by adjusting the integrated opacities for each sightline (Capitanio et al. 2017).

The resulting dust map has a resolution of 5x5x5 parsec cubes and gives the color excess for each cube. The errors on the distance are high compared to the size of the cubes. Still the resolution of the map is better than of any previous map. In the map the color excess E_{B-V} per parsec for that particular cube is given. So the values of the cubes have to be added up to get the total color excess.

The dust map is available at `https://stilism.obspm.fr/about` and I retrieved it on 6th May 2019.

On the webpage there is also an online tool with which the data can be retrieved. When the Galactic coordinates of a sightline are entered the reddening is shown up to a certain distance dependent on the sightline. Only one sightline at a time can be entered and it will be only used for crosschecking here.

In Figure 5 the dust map used in this work is shown. The Galactic plane can be recognised as well as the Bulge.
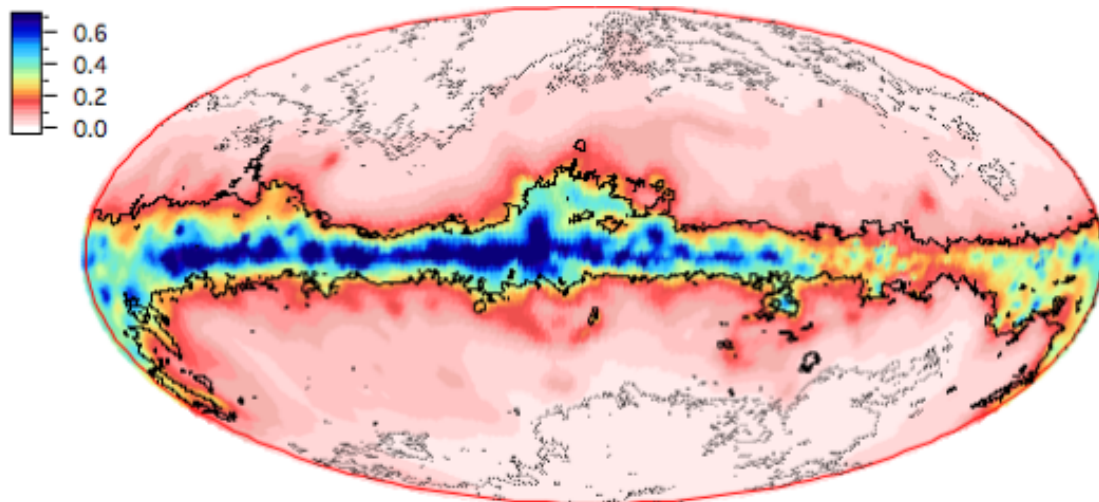

Figure 5: Interstellar dust map (Capitanio et al. 2017)

7   Method

To allow for the automatic access to the dust map using large target lists, I developed my own tool in this work. I used Python 3.7 in a Jupyter notebook (version 5.4.0) provided by the Anaconda distribution (version 1.9.7) and the following packages:

- math

- itertools

- h5py (version 2.9.0)

- numpy (version 1.14.2)

- pandas (version 0.22.0)

- astropy (version 3.2.1)

- matplotlib (version 2.1.2)

The coordinates in the hot subdwarf catalog are given in right ascension and declination but the dust map uses Cartesian coordinates. So the first step was to convert the coordinates from the hot subdwarf catalog into Cartesian coordinates. Then all the values are read from the file and are written to lists. Since not all stars have B and V apparent magnitude data from APASS all stars which do not have this data are excluded to be able to compare the results when using BP and RP versus using B and V. I then apply the following selection criteria:

- positive parallax

- parallax error $< 20\%$

- $|x| < 2$ kpc and $|y| < 2$ kpc and $|z| < 300$ pc (dimensions of the dust map)

To find out to which cube the position and distance of the star correspond, I defined a number of parallel planes (black lines in example in Figure 6) depending on the coordinate value in the given direction. Those planes represent the sides of the cubes and a line (red in Figure 6) defines the sightline from the Sun to a given star. The calculation of the intersections with a self-defined function, which I took from `https://rosettacode.org/wiki/Find_the_intersection_of_a_line_with_a_plane#Python`, of the line with the planes gives the transitions from one cube to the next.

The intersections are only calculated in the positive direction of each spatial direction. This is possible because the mathematical problem is pointsymmetric with respect to the origin (Sun). So a check of the sign of the coordinate gives the right sign for the intersection points. This is done at a later point.

If the absolute value of x, y or z for a star is smaller than 2.5pc, [0, 0, 0] will be added as an intersection point. This is needed because otherwise the star would not be represented in the list of intersection points for that spatial direction. Because the star would be missing in one of the lists but not the others, the coordinates of intersection points would be mismatched, as soon as the lists of the different spatial directions are merged together.
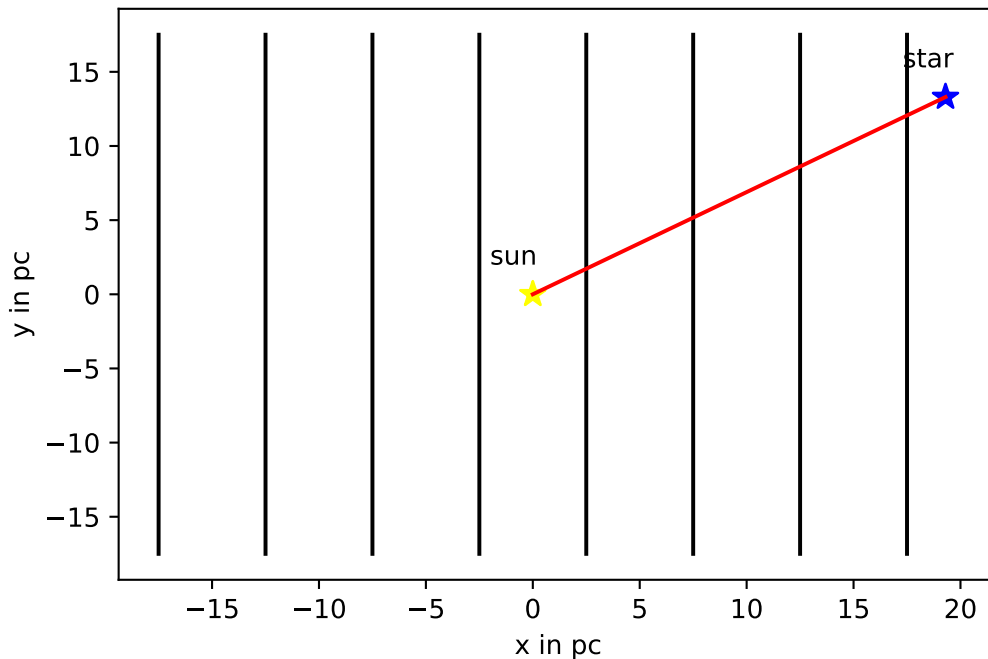
Figure 6: 2D example for the intersection point calculation in x direction, black: Edges of the cubes, red: Line of sight

The intersection points are in one big list, so the next step is to split the list into smaller lists, each list containing the intersection points of only one star. Here also the correction for the wrong sign is made by checking the sign of the coordinates of the star. This is done for all three coordinate directions.

The coordinates of the intersection points of the three directions are put in one list for each star. Now there are three arrays in each list. For simplicity just a list of the coordinates is created. In this list each intersection point is an array but in this case it is easier to work with lists so the arrays are turned into lists. So there is a list of lists with intersection points for each star. Then the intersection points are sorted according to their x values. Herefore a custom sorting key has to be created. This key just returns the absolute value of x since writing abs(x) as sorting key in the sorting function itself doesn't work.

As a next step the numbers of the cubes have to be determined to be able to get the extinction from the map. First the Sun position in the map, which correponds to the cube numbers [399, 399, 59], is added to the cubes in the line of sight. Then each intersection point is checked for which coordinate direction is close to a side of a cube. Here searching close to the cube side is necessary because the calculation of the intersection points is not precise and can give values which lie around 10^{-7} away from the actual value. When the coordinate is close to a side of a cube the sign of the coordinate is checked and then 1 is added to or substracted from the cube number of the spatial direction which coordinate was close to a side of a cube depending on the sign.

The cubes are again in one big list and a list for each star would be better. To achieve this, the number of cubes the light travels through, needs to be known. To calculate this number, the length of the list with the intersection points for each star is taken. But since in the beginning for some stars the origin had to be added to that list, this has to be accounted for here. Then the sublist with the cubes for each star is created and after that the origin is added to those sublists which not yet include it.

The distance travelled through each cube is calculated by taking the length of the vector from one intersection point to the other. Again the result is a big list which has to be divided into sublists, one for each star.

The data from the dust map is read into Python and turned into a numpy array. First the lower and upper errors are retrieved. Lower and upper mean in this case the error below the reddening value and above the reddening value respectively. After that the reddening values of the cubes are retrieved. To obtain the reddening value for a cube for a specific star, the reddening per parsec value is multiplied by the distance the light travels through the cube. The reddening values are in a big list, so again a sublist is made for each star. After that the sum of each individual sublist is computed to get the total reddening of the corresponding star.

First the absolute magnitude is calculated with the Gaia parallax and the apparent G magnitude and is corrected for extinction. Also the lower and upper errors are calculated. Now the color index is corrected for the reddening. Then the absolute magnitude criterion is applied. Those stars that satisfy the criterion are then divided into the three groups for the additional criteria. Those criteria are then tested using BP-RP.

Then the steps beginning from calculating the reddening per cube are repeated. This time not the correct distance through each cube is taken but 5 pc per cube, to see if this makes a considerable difference because calculating the exact distance per cube and exact reddening/extinction might be excessively precise. The dust map has large errors on the cube position compared to the cube size, the reddening values sometimes have large errors as well. Here I want to check, if it is necessary to take the exact distance.

Before the use of the APASS magnitudes new color criteria have to be established. They are derived from the uncorrected color magnitude diagram. Derived from this diagram (see Figure 28) the color critera are:

- for stars with $-1.0 < M_V \leq 4.3 : M_V \geq 7.57 \cdot (B-V) + 2.03$

- for stars with $4.3 < M_V \leq 7.0 : M_V \geq 33.75 \cdot (B-V) - 6.84$

The steps from calculating the absolute magnitude are repeated with the correct distance per cube but now the B and V apparent magnitudes of APASS are used, to check if the error which is made by using BP-RP instead of B and V has to be considered.

8 General results

8.1 Star positons

Only 10378 stars of the whole sample have both B and V magnitude data from APASS. The stars which can be considered here according to the criteria of having a positive parallax and an error smaller than 20% are shown in Figure 7. These are 5504 stars. In Figure 8 all the stars in the dust map limits are shown. Only 1408 stars are within the limits of the dust map. This are only 3.5% of the original size of the catalog and 25.6% of the stars fulfilling the criteria. This sample is therefore small compared to the size of the used catalog and results can not be generalized without consideration of the constraints which have to be made here.

There is a clear pattern how the stars are distributed on the sky. There are two agglomerations of stars one from 0 to about 100 degrees in longitude and the other from around 180 to 250 degrees in longitude. Those are the directions slightly to the side of the Galactic center and the opposite direction, respectively. This distribution of stars looks very different to the larger sample and therefore has some biases. It is not completely clear what causes this selection effect.
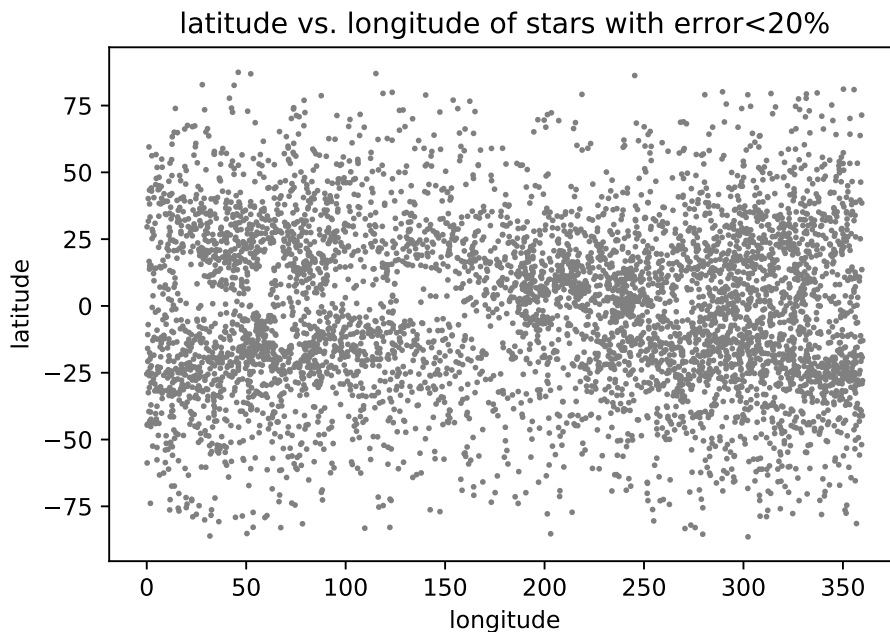
Figure 7: Galactic coordinates of selected stars

Figure 8: Galactic coordinates of selected stars in dust map limits

8.2 Distances

Figure 9: Distance of the stars that are within the dust map limits

The distance distribution in Figure 9 shows a steep increase of the number of stars up to 100 pc. For larger distances the number of stars continually decreases with some small deviations and from 2150 pc on, there are only very few stars. This makes sense because

those stars are situated at the edges of the dust map and therefore the volume in which a star can lie to be in the dust map limits becomes smaller.

9 Results using Gaia distances and magnitudes

9.1 Reddening and extinction

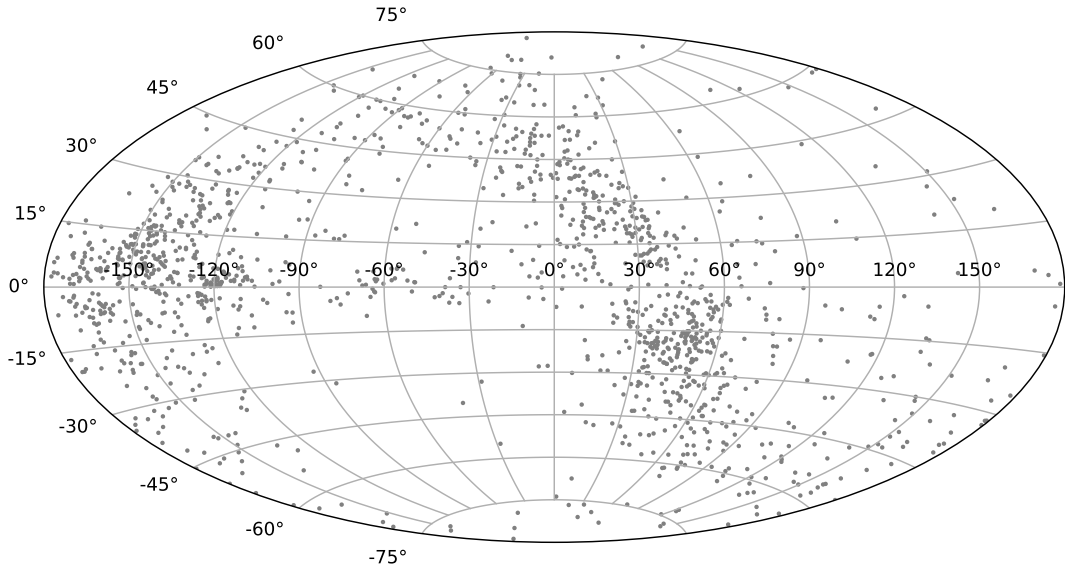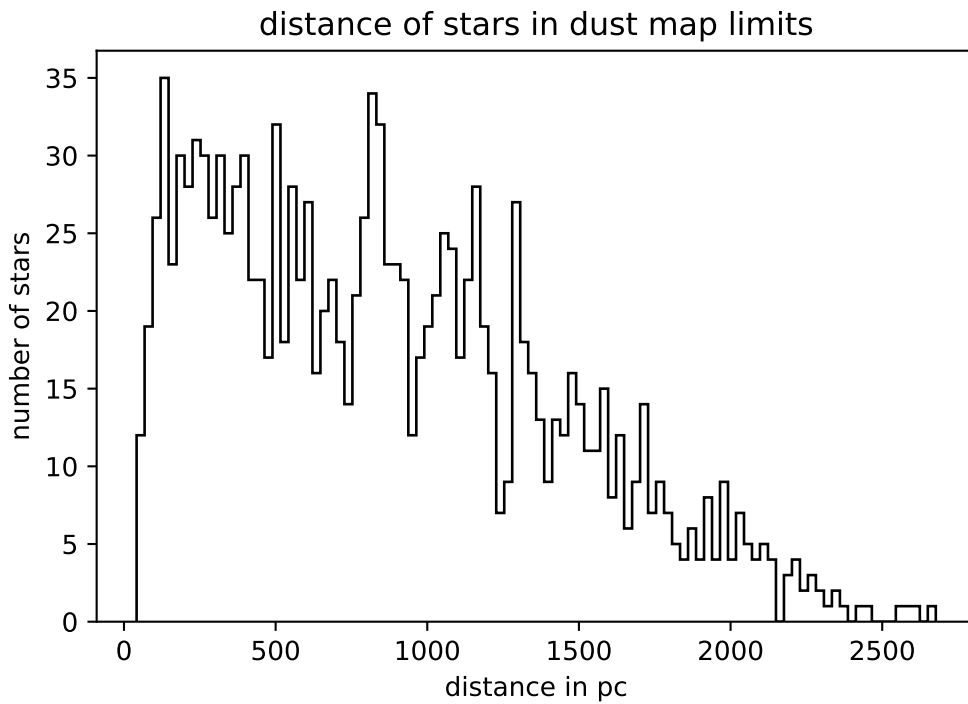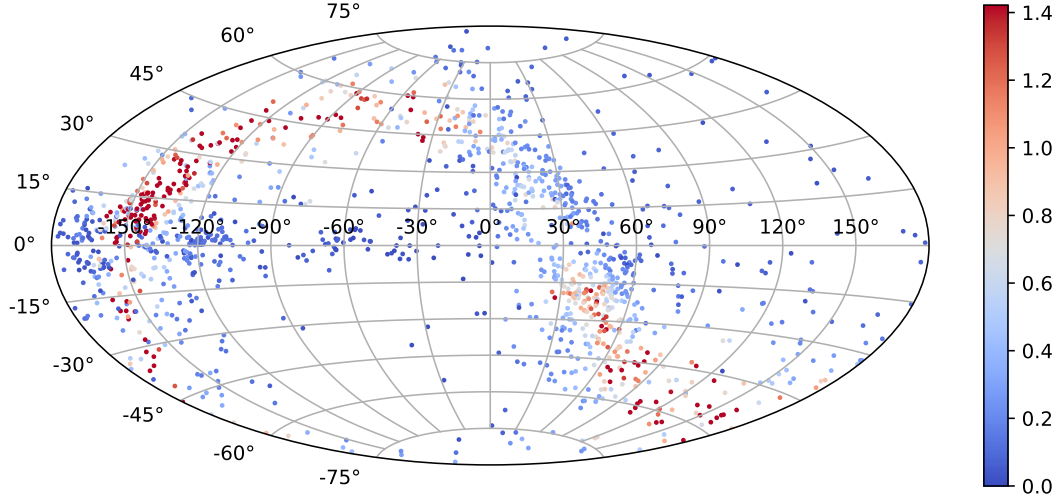Figure 10: Galactic coordinates of the stars in dust map limits with extinction

In Figure 10 the distribution of the stars and their extinction is shown. The highest extinction value displayed is $A_V = 1.4$ and all higher extinction values have the same shade of red. The reason for this display is that there are very few stars which have a high extinction and the vast majority has only low extinction below one.

The high extinction values are not measured at the coordinates where they would be expected. They are not primarily measured in the Galactic plane but they 'follow' the main band where the most stars are located in this sample. This means there have to be clouds of dust in those areas of the sky. I crosschecked random sightlines with the reddening values on the website with the online tool:

$l\,[°]$	$b\,[°]$	distance [pc]	$E_{B-V,calc}$ [mag]	$E_{b_v,5pc}$ [mag]	$E_{B-V,website}$ [mag]
208.931	7.85485	1573.56	0.671 ± 0.075	0.918 ± 0.075	0.06 ± 0.019
82.645	-24.911	420.35	0.079 ± 0.033	0.132 ± 0.033	0.05 ± 0.022
49.760	-11.415	1481.7	0.124 ± 0.13	0.185 ± 0.13	0.118 ± 0.031
214.578	66.392	274.05	0.047 ± 0.028	0.07 ± 0.028	$0.017^{+0}_{-0.023}$
200.176	-4.692	121.85	0.007 ± 0.017	0.009 ± 0.017	0.003 ± 0.016
308.197	2.228	203.21	0.012 ± 0.015	0.019 ± 0.015	0.08 ± 0.021
61.437	-3.629	273.37	0.038 ± 0.025	0.061 ± 0.025	0.034 ± 0.028

Table 1: Crosschecks of random stars with the online tool of the website

Unfortunately the online tool shows for Galactic latitudes which are higher than around $|b| > 25°$ only reddening values for a few hundred parsec. The crosscheck shows that most of the reddening values are within errors but it also shows that the errors are high most of the times especially if the sightline is not towards the Galactic center.

There are some stars for which the reddening correction didn't work. They have unrealistically high reddening values. The color excess for the hottest stars known does not exceed $B - V = -0.7$. Stars with de-reddened $B - V < -0.7$ have therefore been excluded.

9.2 Applying absolute magnitude and color excess criteria

Only 1184 of the 1408 stars pass the color excess criterion of $B - V > -0.7$. The other stars have a bluer color and are therefore excluded because the reddening correction did not work. The absolute magnitude criterion $-1.0 < M_G < 7.0$ is satisfied by 1184 of the 1184 stars. All stars pass this criterion because those stars which have a very high extinction and might fail this criterion were excluded in the step before. Here the G magnitude is used as the visual magnitude of the stars and the E_{B-V} of the dust map is used as the color excess.

The color criteria are satisfied by all 1184 stars. Again those stars which might fail at this criterion were excluded at the beginning.

All stars which are excluded are excluded because of them becoming too blue. For 15.9% of the stars the reddening correction did not work.

In Figure 11 the color magnitude diagram of the 1408 stars is displayed. The grey dots resemble the stars which satisfy the criteria and the red dots those stars which don't. Figure 12 shows the color magnitude diagram before the correction for reddening and extinction. The stars which do not satisfy the criteria are shown in red to show where the stars were in the diagram before correction. Most of those stars are close to the border of the $B - V > -0.7$ criterion. When the color magnitude diagrams before and after correction are compared, the movement of the stars in the diagram can be seen. The stars move up and to the left to brighter magnitudes and bluer colors. The main features of the distribution of the stars in the diagram before the correction can be found in the diagram after the correction. For example the agglomeration of stars in the area of $M_G \approx 4$ and $BP - RP \approx -0.5$. Also the border of the criteria towards the main sequence is visible.

This also means that all stars, for which the reddening correction worked, can still be considered hot subdwarf star candidates.

In Figure 13 a map of the stars is shown. The red dots are stars which do not satisfy the criteria. Those stars are at those positions on the map where, according to the dust map, the extinction is highest. Only some of the stars are in the Galactic plane but most of them are in the 'band' of stars.

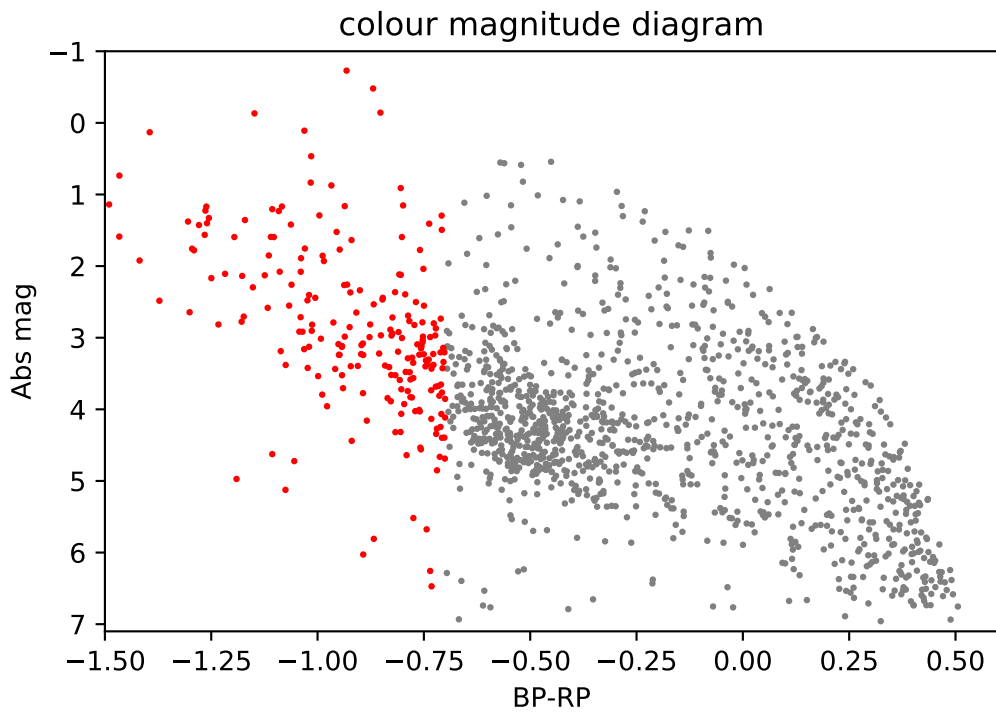Figure 11: Color magnitude diagram, red: Unselected stars, grey: Stars which satisfy the criteria
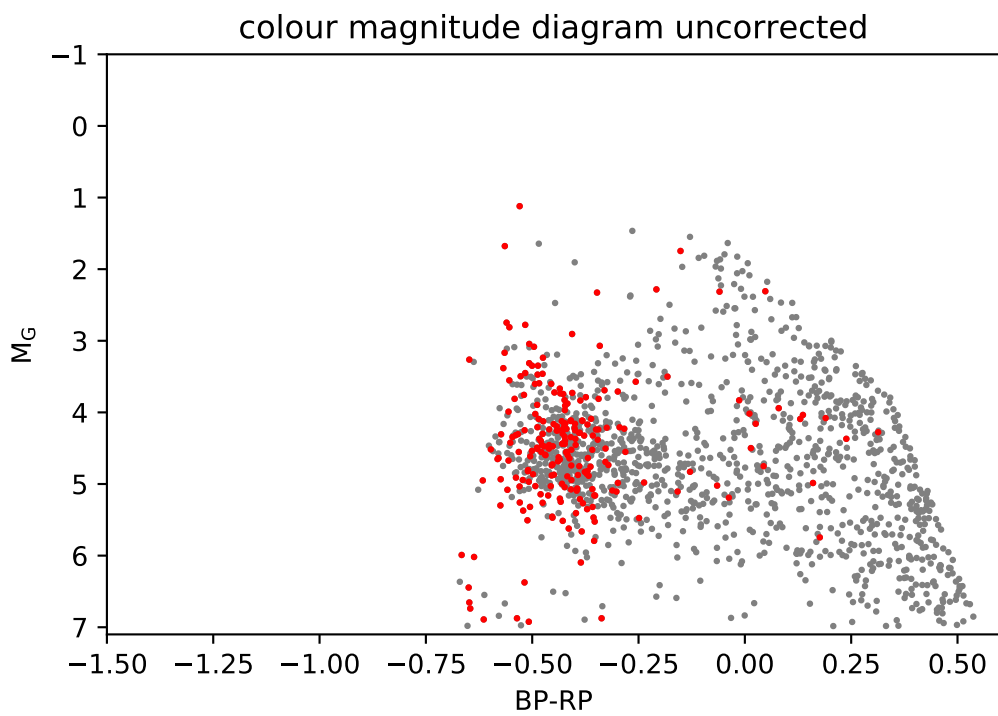

Figure 12: Color magnitude diagram before the correction for reddening, red: Unselected stars, grey: Stars which satisfy the criteria
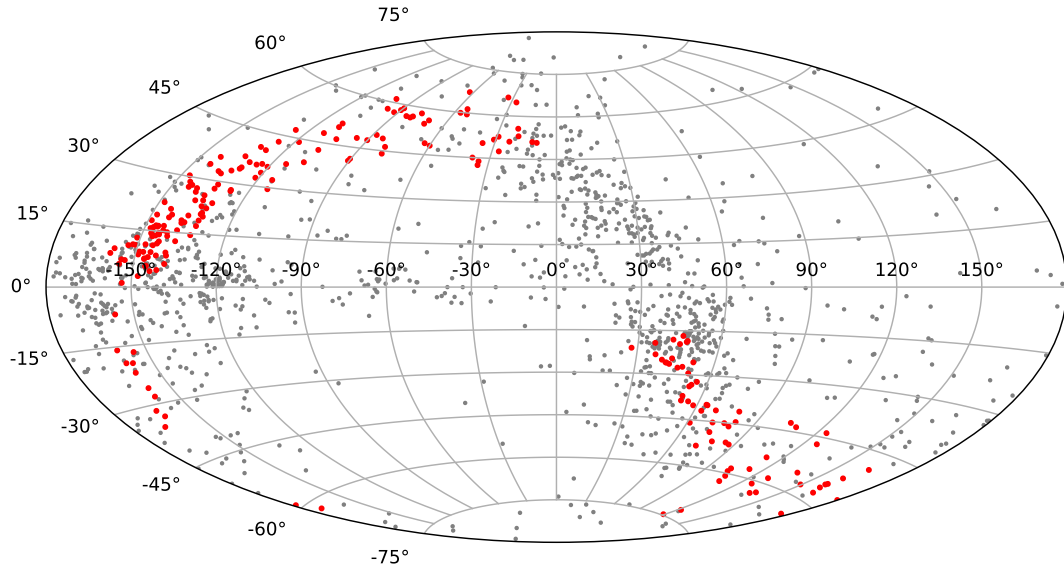
Figure 13: Map of the stars in Galactic coordinates, grey: Stars satisfying the criteria, red: Unselected stars
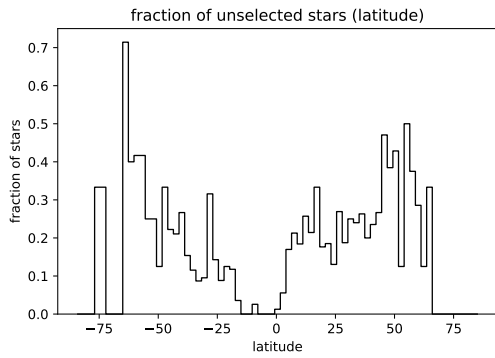
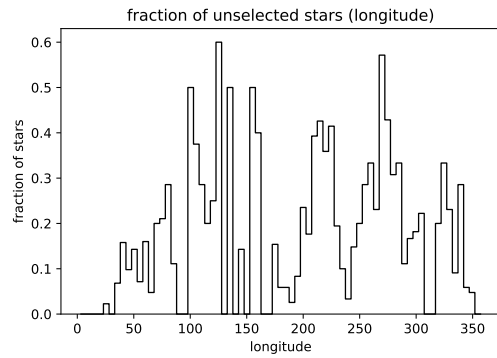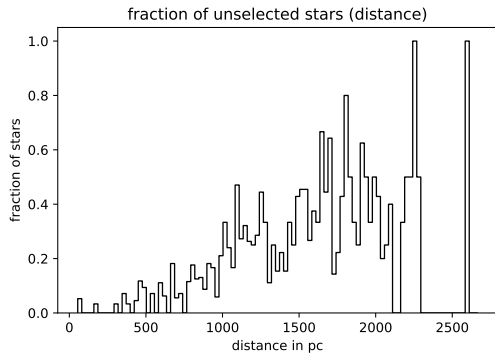## 9.3 Statistics

Figure 14

Figure 15

Figure 16
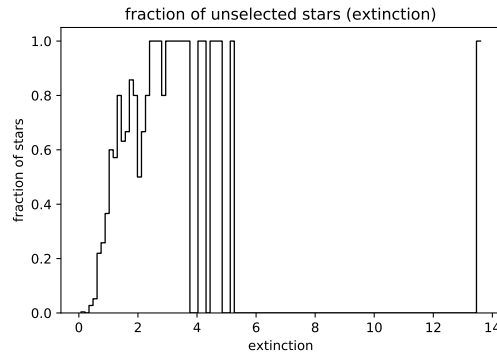
Figure 17

Above are some statistics for the stars, which did not satisfy the criteria. In Figure 14 the fraction of stars which are not selected against Galactic latitude is shown. In the Galactic plane there are nearly no stars which fall outside of the criteria. For higher latitudes this fraction becomes higher. This result is unexpected since the reddening in the Galactic plane should be larger and therefore the correction should be stronger but the stars for which the reddening correction did not work lie outside of the Galactic plane.

Figure 15 shows the same as Figure 14 but for the Galactic longitude. The distribution of the stars not satisfying the criteria is random. Noteworthy is that there are no stars in the direction to the Galactic center excluded. This is again very unexpected for the aforementioned reason. Also in the anti-center direction there is a smaller fraction of stars excluded.

In Figure 16 the distance distribution of the fraction of unselected stars is shown. It shows clearly that for large distances many stars are not selected. It was expected that for large distances the rate of not selected stars is high because the distance is large and there may be many clouds in the sightline. A higher fraction for the stars with short distances was expected because in the close vicinity of the Sun, the thin disk, are many blue main sequence stars, so some misclassifications were expected.

The fraction of not selected stars against their extinction is plotted in Figure 17. This is completely as expected. The stars with high extinction are more likely not to fulfill the criteria of being a hot sudwarf than those with low extinction. The smaller the extinction value becomes the smaller is the fraction of not selected stars.

10 Results using 5pc per cube and Gaia magnitudes

10.1 Reddening and extinction
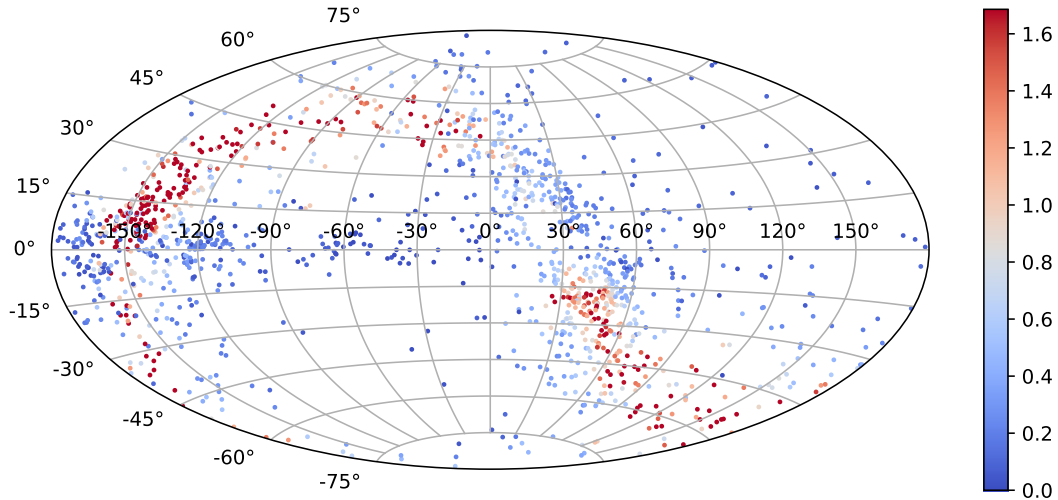
Figure 18: Galactic coordinates of stars in dust map limits with extinction

Figure 18 shows the position of the stars on the sky in Galactic coordinates and their calculated extinction when every cube the line of sight passes is counted with 5 pc, which is the length of the side of a cube. The maximum extinction value of the colorbar is $A_V = 1.7$ to better show the extinction of the majority of stars because there are few stars with very high extinction and the majority has low extinction values.

The distribution has not changed in comparison to using the correct distance, but the extinction is stronger. Still the extinction is not the highest in the galactic plane but in the band where the most stars are.

10.2 Applying absolute magnitude and color excess criteria

When calculating the reddening with 5pc per cube only 1098 of 1408 stars are satisfying the first color criterion. This are 86 stars more than when using the correct distance per cube. This result is not surprising because the reddening got higher for each star. The absolute magnitude criterion of $-1.0 < M_G < 7.0$ is satisfied by all the remaining stars.

All remaining stars satisfy the color criteria. As for the first method those stars which would not pass the absolute magnitude and color criteria are already excluded in the first step.

The color magnitude diagram after the reddening correction is shown in Figure 19. The stars which satisfy the criteria are plotted in grey and those that do not in red. In general this color magnitude diagram is stretched towards brighter and bluer stars in comparison

to the color magnitude diagram when using the correct distance. Which means there are more bright and blue stars than before. The color magnitude diagram before the correction is in Figure 20. Here many of the stars which are already blue before the reddening correction are excluded because they wander towards too blue colors. Again there are no stars which wander towards the main sequence but all stars are becoming bluer and brighter.

The map of the stars is shown in Figure 21. The distribution looks much like in the case of calculating the reddening with the correct distance per cube. Again there are no stars in the Galactic plane but in the 'band' of stars.
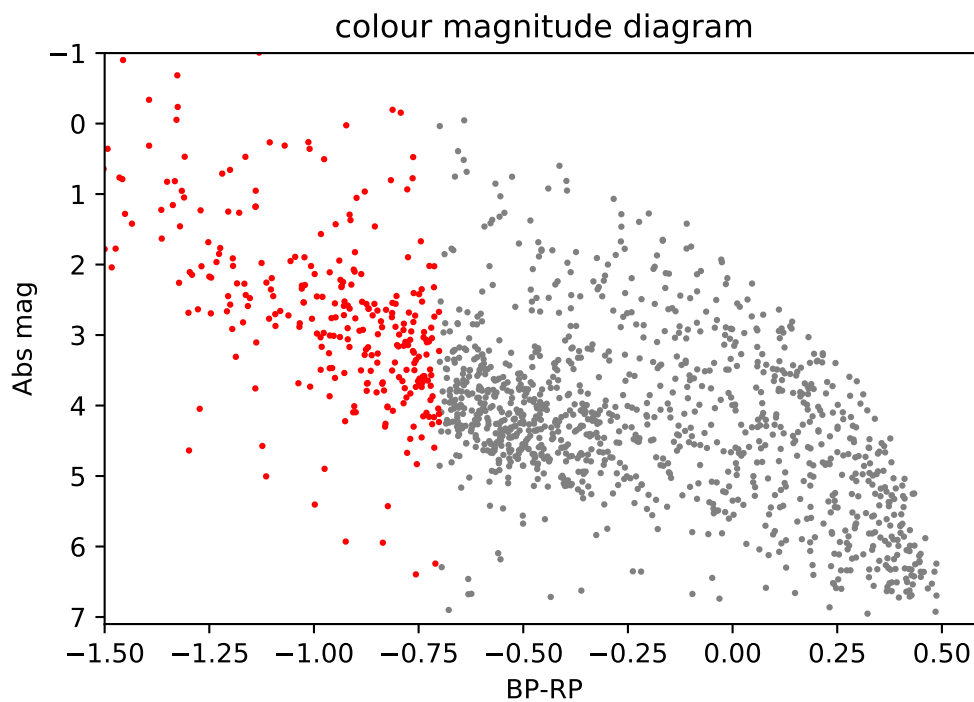
Figure 19: Color magnitude diagram after reddening correction with 5 pc per cube, grey: Stars satisfying the criteria red:Unselected stars
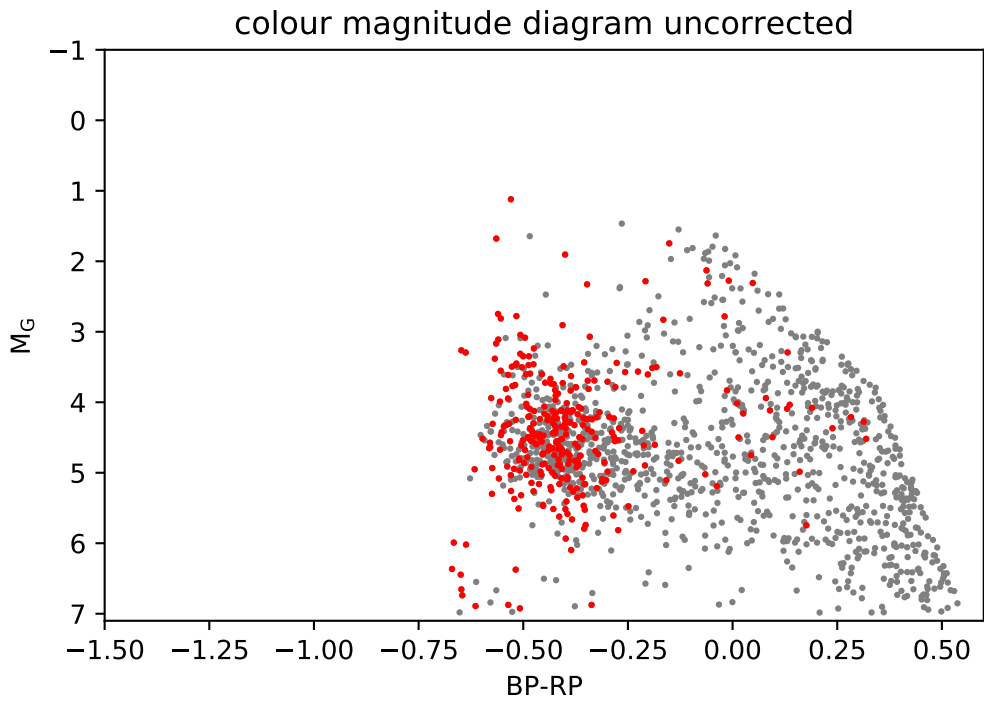
Figure 20: Color magnitude diagram before the reddening correction, grey: Stars satisfying criteria, red: Unselected stars
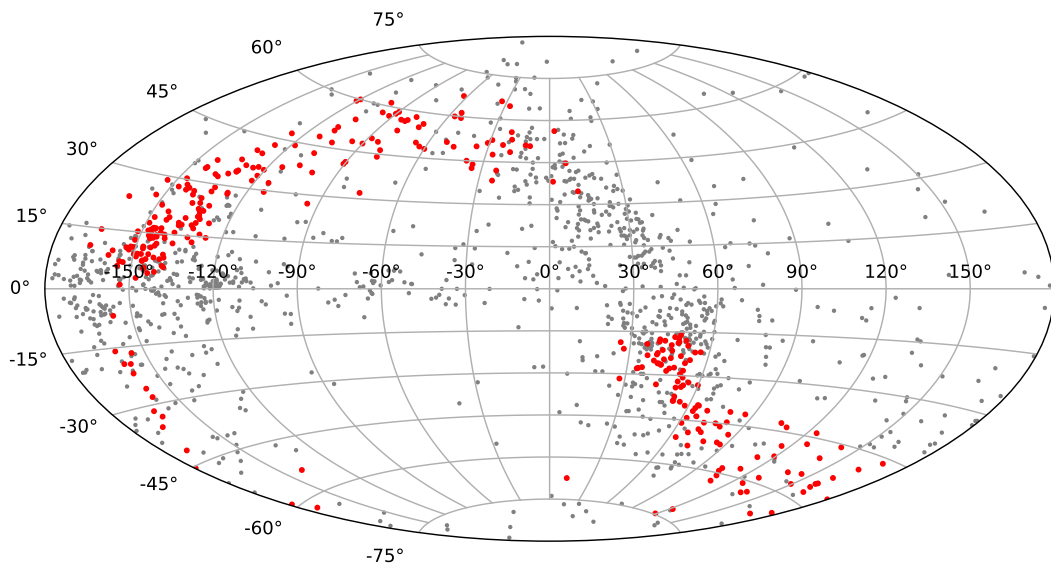
Figure 21: Galactic coordinates, grey: Stars satisfying criteria, red: Unselected stars

10.3 Statistics
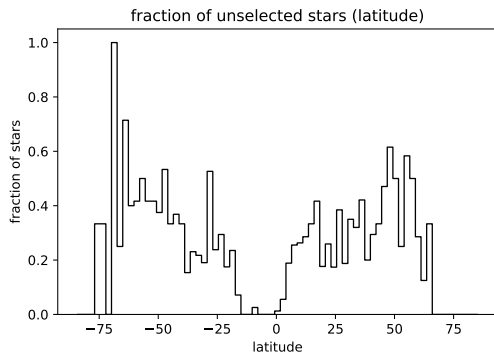
Figure 22
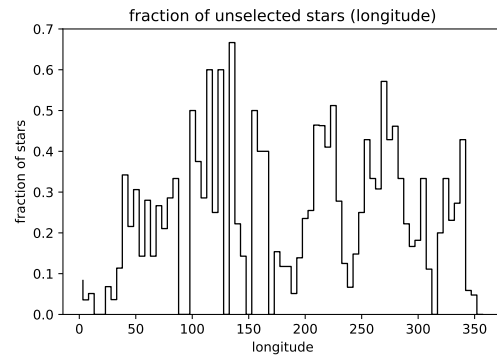
Figure 23
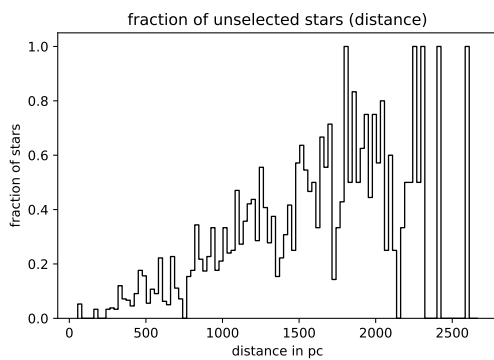
Figure 24
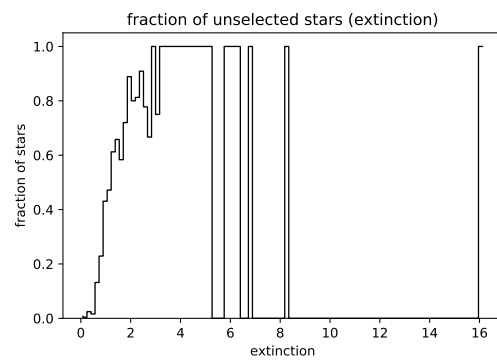
Figure 25

Figure 22 shows the fraction of stars which do not satisfy the criteria plotted against the Galactic longitude. The highest fraction is at high latitudes so like in the first method outside of the Galactic plane.

The fraction of stars against the longitude (Figure 23) shows a similar distribution as the first method. The fraction is higher because in total more stars are excluded but the distribution stays the same.

The distance distribution of the fraction of stars is shown in Figure 24. Here stars lying further away have a higher fraction of not fulfilling the criteria.

The fraction of stars versus the extincion is shown in Figure 25. The extinction is very high for some stars. Also those stars with high extinction are excluded from the subdwarf selection and the percentage goes down for lower extinctions.

11 Results using Gaia distance and APASS magnitudes

11.1 Reddening and extinction
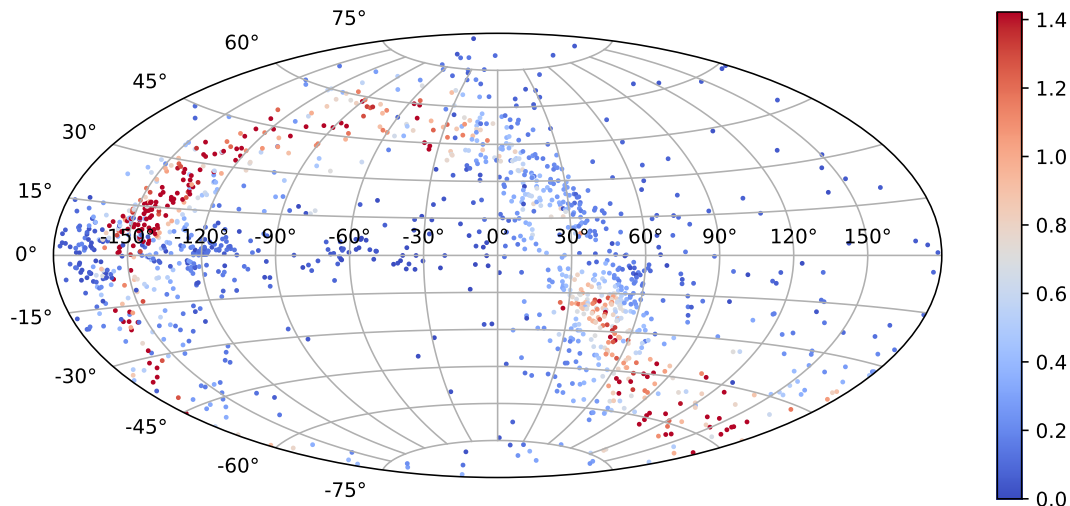
Figure 26: Galactic coordinates with extinction

Figure 26 shows the position on the sky and the extinction for the stars. As before the maximum extinction value is $A_V = 1.4$ to highlight the extinction distribution at low extinction values.

The extinction distribution has not changed in comparison to the other two calculation methods.

11.2 Applying absolute magnitude and color excess criteria

For the calculation with B and V magnitudes I used the absolute magnitude criterion as before but I derived own color selection criteria based on the distribution of stars before the correction (see Figure 28). I have only two brightness classes because there were not many bright stars with which I could have derived a criterion for bright stars. The two brightness classes have roughly the same amount of stars.

First the stars with too blue colors are excluded. These are 89 stars, so for 1319 stars the reddening correction worked. After that the absolute magnitude criterion is applied. This criterion is satisfied by all remaining stars.

The color criteria are satisfied by 1279 stars. This means that 40 stars do not satisfy the criteria. Two thirds of the stars not satisfying criteria are in the brighter class, the other third are in the dimmer class. In contrast to the other two methods, using the B and V magnitudes stars are excluded by the color criteria.

The comparison of the color magnitude diagrams before (Figure 27) and after (Figure 28) the correction shows that the stars wandered towards smaller magnitudes and bluer B-V. There are some stars which are excluded because of their position in the color magnitude diagram even before correction by just applying the selection criteria. These stars are probably blue main sequence stars which found their way into the hot subdwarf candidate list.

The map of the stars show that the stars not satisfying the $B - V > -0.7$ criterion are the same as in the other two methods and lie in the stellar 'band' but here also several stars are in the Galactic plane which would be expected.
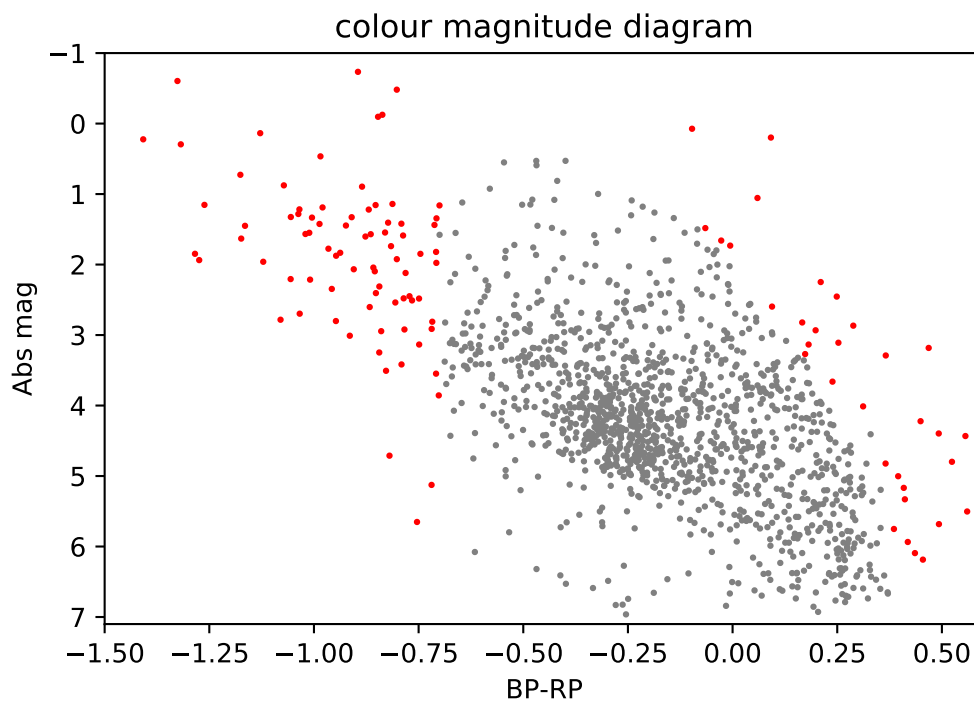
Figure 27: Color magnitude diagram with B and V magnitudes, red: Unselected stars, grey: Selected stars
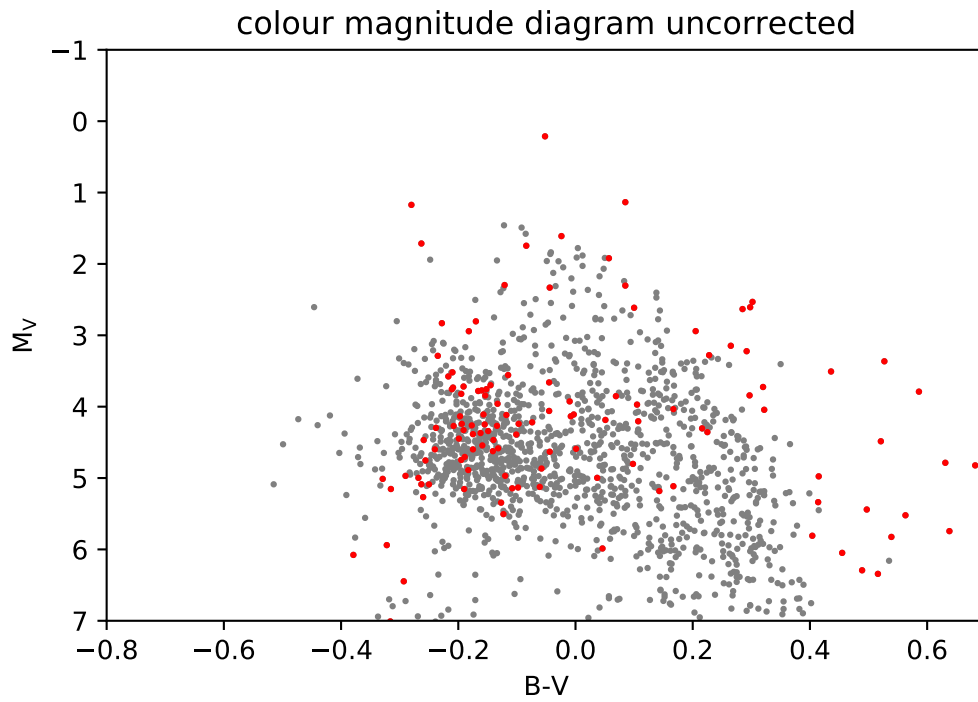
Figure 28: Color magnitude diagram before the extinction correction and with B and V magnitudes, red: Unselected stars, grey: Selected stars
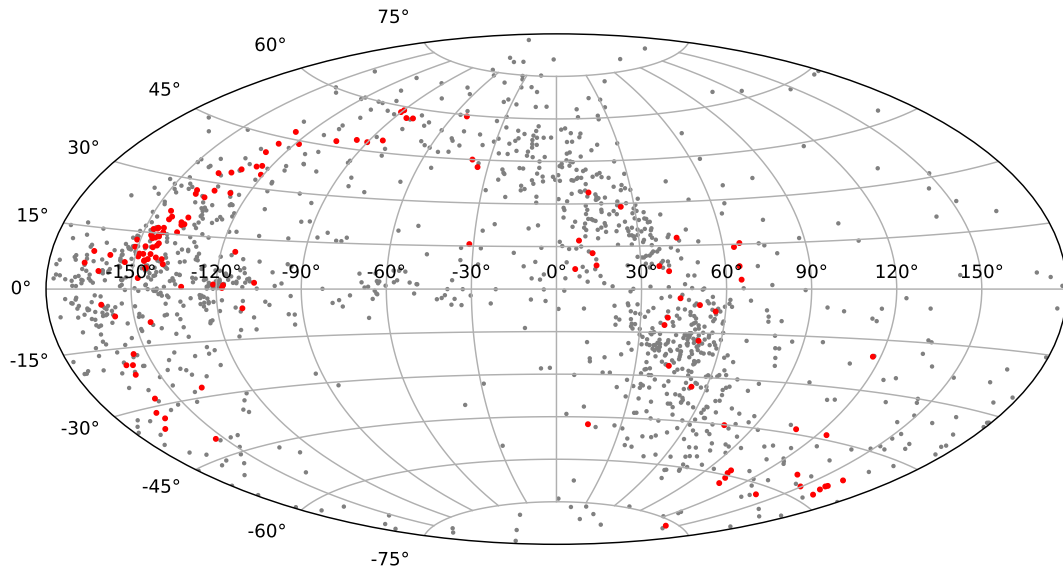
Figure 29: Galactic coordinates with B and V magnitudes, red:Unselected stars, grey: Selected stars

11.3 Statistics

fraction of unselected stars (latitude)

Figure 30

fraction of unselected stars (longitude)

Figure 31

fraction of unselected stars (distance)

Figure 32

fraction of unselected stars (extinction)
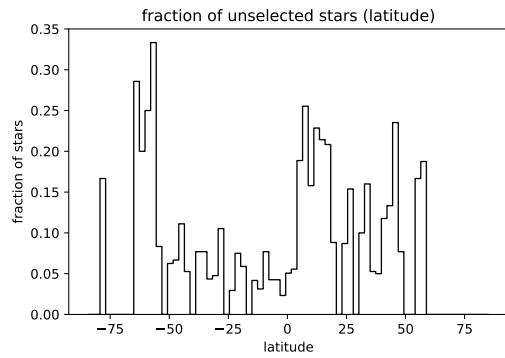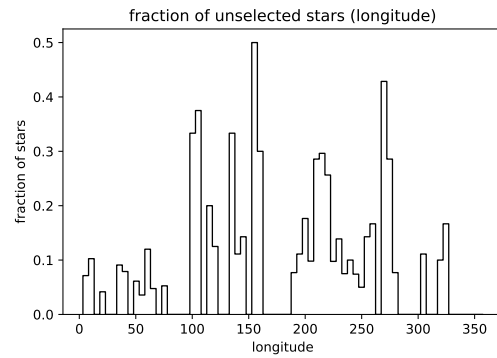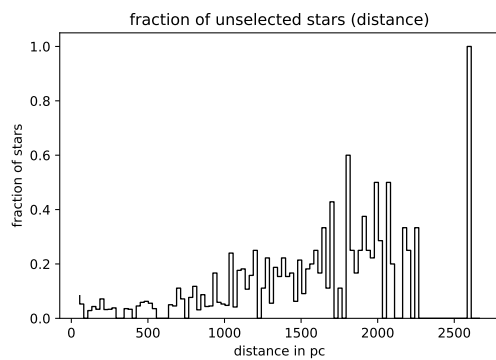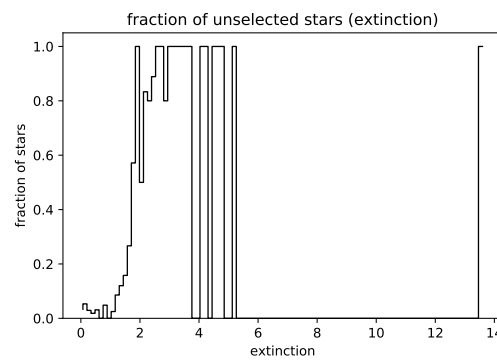
Figure 33

For the latitude the highest fraction of stars not satisfying the criteria is still outside the Galactic plane as shown in Figure 30 but there are now also stars that are in the Galactic plane and do not fulfill the criteria.

The fraction distribution versus longitude is shown in Figure 31. It looks different from the results of the other methods because there is a high fraction of stars not satisfying the criteria near the Galactic anti-center direction but in the exact anti-center direction the fraction is small again. Also the fraction of stars near or in the direction of the Galactic center is small compared to the other two methods.

With respect to the distance (Figure 32) the fraction is smaller than for the other methods. Especially for far away stars the fraction is smaller. The general trend of a decreasing fraction towards short distances is still there.

Figure 33 shows the fraction of excluded stars versus extinction. The fraction is large for higher extinction and becomes smaller for lower extinction similar to the other methods.

12 Conclusions

I calculated the reddening and extinction corrected absolute magnitude and color index of 1408 hot subdwarfs from the Gaia hot subdwarf catalog using three different methods. I used a new dust map for the reddening values and Gaia and APASS magnitudes to calculate the extinction corrected values.

The stars in the limits of the dust map are distributed sinusoidally in Galactic coordinates and not along the Galactic plane. This is the result of some kind of selection effect which is not yet known.

The distances were computed with Gaia parallaxes better than 20% and should therefore be very precise. They show a linear decrease of the amount of stars per distance interval from 100 pc on.

The correction for extinction shows that all of the hot subdwarf candidates that pass the color cut also satisfy the subdwarf criteria when using the Gaia magnitudes and the correct distance per cube. Those stars not surviving the color cut, 15.9% of the stars, are the stars with the highest extinctions and they are at higher distances. They are not in the Galactic plane as expected.

When using the Gaia magnitudes and calculating the extinction per cube with 5 pc per cube all of the candidates satisfying the first color cut also satisfy the other criteria. Those not surviving are again those with high extinction and they are at high distances. This time there are 22% of the stars not surviving the color cut. They are distributed similar as before.

In the last method the Gaia distance per cube is used again, but this time APASS magnitudes. With this method 6.3% of the stars do not pass the color cut. They are at similar positions as in the other two methods and again at high distances and with high extinction. Applying the color criteria derived by myself an additional 40 stars, corresponding to 3% of the stars, are not satisfying the color criteria. These stars are in the Galactic plane where some misclassifications were expected.

For all methods the main latitude values of the stars which are not selected are outside the Galactic plane. Also strong extinction sightlines and more distant stars have a higher fraction of unselected stars.

The difference between using Gaia distances and 5 pc per cube is that 6% more stars do not pass the color cut of $B - V > -0.7$. For those stars passing the color cut there is no difference between the two methods when applying the absolute magnitude and the color criteria.

There is a larger difference between using Gaia filters or B and V of the Johnson filter system. The color magnitude diagrams already have some differences with some stars not satisfying the color criteria even prior to the correction when using the Johnson filter magnitudes. Also 9.6% more stars survive the color cut at the beginning when using the

Johnson filter magnitudes. So there is a difference between these two filter systems. Since the reddening of the dust map is given in the Johnson filter system the Gaia filter system is more prone to error than the APASS magnitudes.

There are some strange selection effects when applying the parallax error criterion and only selecting the stars in the dust map limits. The distribution of the stars is not as expected. Also the regions with high reddening are not primarily in the Galactic plane but in the areas in which the most of the selected stars are. These two instances can not really be explained but with more advanced dust maps with a smaller error on distance and the reddening, better results might be achieved. In the next data releases of Gaia the distances and apparent magnitudes of the filters will be improved as well. Also the selection criteria for the hot subdwarf candidates were empirically derived and can be further improved. They also depend on the filter system.

In this work no stars which were not yet included as candidates were investigated. Some of those redder stars which are not yet candidates might fulfill the selction criteria of subdwarfs when their magnitude and color index are properly corrected. This is the topic of further research.

References

[1] L. D. Anderson, T. M. Bania, D. S. Balser, V. Cunningham, T. V. Wenger, B. M. Johnstone, and W. P. Armentrout. The wise catalog of galactic HII regions. *Astrophysical Journal, Supplement Series*, 212(1), 2014.

[2] J. Blanchette, P. Chayer, F. Wesemael, G. Fontaine, M. Fontaine, J. Dupuis, J. Kruk, and E. Green. FUSE Determination of Abundances in Long-Period Pulsating V1093 Her (PG 1716+426) Stars1 . *The Astrophysical Journal*, 678(2):1329–1341, 2008.

[3] W. R. Brown, J. Anderson, O. Y. Gnedin, H. E. Bond, M. J. Geller, and S. J. Kenyon. Proper motions and trajectories for 16 extreme runaway and hypervelocity stars. *Astrophysical Journal*, 804(1):49, 2015.

[4] G. Busso, S. Moehler, M. Zoccali, U. Heber, and S. K. Yi. Hot subdwarfs in the Galactic bulge. *Baltic Astronomy*, 2006.

[5] L. Capitanio, R. Lallement, J. L. Vergely, M. Elyajouri, and A. Monreal-Ibero. Three-dimensional mapping of the local interstellar medium with composite data. 65, 2017.

[6] S. Cassisi, H. Schlattl, M. Salaris, and A. Weiss. First Full Evolutionary Computation of the Helium Flash-induced Mixing in Population II Stars. *The Astrophysical Journal*, 582(1):L43–L46, 2003.

[7] X. Chen, Z. Han, J. Deca, and P. Podsiadlowski. The orbital periods of subdwarf b binaries produced by the first stable roche lobe overflow channel. *Monthly Notices of the Royal Astronomical Society*, 434(1):186–193, 2013.

[8] R. A. Chevalier. The Evolution of Supernova Remnants. Spherically Symmetric Models. *The Astrophysical Journal*, 1974.

[9] C. M. Copperwheat, L. Morales-Rueda, T. R. Marsh, P. F. Maxted, and U. Heber. Radial-velocity measurements of subdwarf B stars. *Monthly Notices of the Royal Astronomical Society*, 415(2):1381–1395, 2011.

[10] D. W. Evans, M. Riello, F. De Angeli, J. M. Carrasco, P. Montegriffo, C. Fabricius, C. Jordi, L. Palaversa, C. Diener, G. Busso, C. Cacciari, F. V. Leeuwen, P. W. Burgess, M. Davidson, D. L. Harrison, S. T. Hodgkin, E. Pancino, P. J. Richards, G. Altavilla, L. Balaguer-Núñez, M. A. Barstow, M. Bellazzini, A. G. Brown, M. Castellani, G. Cocozza, F. De Luise, A. Delgado, C. Ducourant, S. Galleti, G. Gilmore, G. Giuffrida, B. Holl, A. Kewley, S. E. Koposov, S. Marinoni, P. M. Marrese, P. J. Osborne, A. Piersimoni, J. Portell, L. Pulone, S. Ragaini, N. Sanna,

D. Terrett, N. A. Walton, T. Wevers, and A. Wyrzykowski. Gaia Data Release 2: Photometric content and validation. *Astronomy and Astrophysics*, 2018.

[11] E. Fitzpatrick. Correcting for the Effects of Interstellar Extinction. *Publications of the Astronomical Society of the Pacific*, 111(755):63–75, jan 1999.

[12] E. L. Fitzpatrick. Interstellar Extinction in the Milky Way Galaxy. 2004.

[13] S. Geier, U. Heber, P. Podsiadlowski, H. Edelmann, R. Napiwotzki, T. Kupfer, and S. Müller. Hot subdwarf stars in close-up view. *Astronomy and Astrophysics*, 519: A25, 2010.

[14] S. Geier, V. Schaffenroth, H. Drechsel, U. Heber, T. Kupfer, A. Tillich, R. H. Østensen, K. Smolders, P. Degroote, P. F. Maxted, B. N. Barlow, B. T. Gänsicke, T. R. Marsh, and R. Napiwotzki. Binaries discovered by the MUCHFUSS project: SDSS J08205+0008 - An eclipsing subdwarf B binary with a brown dwarf companion. *Astrophysical Journal Letters*, 731(2 PART II), 2011.

[15] S. Geier, R. H. Østensen, P. Nemeth, N. P. Gentile Fusillo, B. T. Gänsicke, J. H. Telting, E. M. Green, and J. Schaffenroth. The population of hot subdwarf stars studied with Gaia: I. the catalog of known hot subdwarf stars. *Astronomy and Astrophysics*, 600, apr 2017.

[16] S. Geier, R. H. Ostensen, P. Nemeth, U. Heber, N. P. Gentile Fusillo, B. T. Gänsicke, J. H. Telting, E. M. Green, and J. Schaffenroth. Meet the family the catalog of known hot subdwarf stars. *Open Astronomy*, 26(1):164–168, 2017.

[17] S. Geier, R. Raddi, N. P. G. Fusillo, and T. R. Marsh. The population of hot subdwarf stars studied with Gaia II. The Gaia DR2 catalogue of hot subluminous stars. (2017): 1–13, 2018.

[18] S. Geier, R. Raddi, N. P. Gentile Fusillo, and T. R. Marsh. The population of hot subdwarf stars studied with Gaia: II. the Gaia DR2 catalogue of hot subluminous stars. *Astronomy and Astrophysics*, 621:1–13, 2019.

[19] J. A. Graham. UBVRI standard stars in the E-regions. Technical report, 94.

[20] Z. Han, P. Podsiadlowski, P. F. Maxted, and T. R. Marsh. The origin of subdwarf B stars - II. *Monthly Notices of the Royal Astronomical Society*, 341(2):669–691, may 2003.

[21] T. I. Hasegawa, E. Herbst, and C. M. Leukng. Models of gas-grain chemistry in dense interstellar clouds with complex organic molecules. *The Astrophysical Journal Supplement Series*, 82:167, 1992.

[22] U. Heber. The atmosphere of subluminous B stars. *Astronomy and Astrophysics*, 155:33–45, 1986.

[23] U. Heber. Hot Subdwarf Stars. *Annual Review of Astronomy and Astrophysics*, 47 (1):211–251, sep 2009.

[24] U. Heber. Hot subluminous stars. *Publications of the Astronomical Society of the Pacific*, 128(966):1–86, 2016.

[25] L. M. Hobbs, D. G. York, J. A. Thorburn, T. P. Snow, M. Bishof, S. D. Friedman, B. J. McCall, T. Oka, B. Rachford, P. Sonnentrucker, and D. E. Welty. Studies of the diffuse interstellar bands. III. HD 183143. *Astrophysical Journal*, 705(1):32–45, 2009.

[26] A. Kawka, S. Vennes, S. O'Toole, P. Németh, D. Burton, E. Kotze, and D. A. Buckley. New binaries among UV-selected, hot subdwarf stars and population properties. *Monthly Notices of the Royal Astronomical Society*, 450(4):3514–3548, 2015.

[27] T. Kupfer, S. Geier, U. Heber, R. H. Østensen, B. N. Barlow, P. F. Maxted, C. Heuser, V. Schaffenroth, and B. T. Gänsicke. Hot subdwarf binaries from the MUCHFUSS project: Analysis of 12 new systems and a study of the short-period binary population. *Astronomy and Astrophysics*, 2015.

[28] K. B. Kwitter, R. H. Méndez, M. Peña, L. Stanghellini, R. L. Corradi, O. De Marco, X. Fang, R. B. Henry, A. I. Karakas, X. W. Liu, J. A. López, A. Manchado, and Q. A. Parker. The present and future of planetary nebula research. A white paper by the IAU planetary nebula working group. *Revista Mexicana de Astronomia y Astrofisica*, 50(2):203–223, 2014.

[29] R. Lallement, L. Capitanio, L. Ruiz-Dern, C. Danielski, C. Babusiaux, L. Vergely, M. Elyajouri, F. Arenou, and N. Leclerc. Three-dimensional maps of interstellar dust in the Local Arm: Using Gaia, 2MASS, and APOGEE-DR14. *Astronomy and Astrophysics*, 616, aug 2018.

[30] T. Lanz, T. M. Brown, A. V. Sweigart, I. Hubeny, and W. B. Landsman. Flash Mixing on the White Dwarf Cooling Curve: Far Ultraviolet Spectroscopic Explorer Observations of Three He-rich sdB Stars . *The Astrophysical Journal*, 602(1):342–355, 2004.

[31] J. W. Lee, S. L. Kim, C. H. Kim, R. H. Koch, C. U. Lee, H. I. Kim, and J. H. Park. The sdB+M eclipsing system HW virginis and its circumbinary planets. *Astronomical Journal*, 137(2):3181–3190, 2009.

[32] P. F. Maxted, T. R. Marsh, and R. C. North. KPD 1930+2752: A candidate type Ia supernova progenitor. *Monthly Notices of the Royal Astronomical Society*, 317(3): 41–44, 2000.

[33] T. J. Millar. Astrochemistry. *Plasma Sources Science and Technology*, 24:010101, feb 2015.

[34] M. M. Miller Bertolami, L. G. Althaus, K. Unglaub, and A. Weiss. Modeling He-rich subdwarfs through the hot-flasher scenario. 2009.

[35] S. Moehler, T. Richtler, K. de Boer, R. Dettmar, and U. Heber. Hot subluminous stars at high galactic latitudes. I, Spectra and Strömgren photometry. *Astronomy & astrophysics. Supplement Series (Print)*, 1990.

[36] R. H. Østensen. The subdwarf database: Released. *Baltic Astronomy*, 15(1):85–90, 2006.

[37] B. Paczynski. Common Envelope Binaries. *Symposium - International Astronomical Union*, 1976.

[38] F. Palla and S. W. Stahler. Star Formation in the Orion Nebula Cluster. *The Astrophysical Journal*, 525(2):772–783, 1999.

[39] F. Salama, G. A. Galazutdinov, J. Krellowski, L. Biennier, Y. Beletsky, and I. O. Song. Polycyclic aromatic hydrocarbons and the diffuse interstellar bands: A survey. *Astrophysical Journal*, 728(2), 2011.

[40] P. A. Van Hoof, G. C. Van De Steene, M. J. Barlow, K. M. Exter, B. Sibthorpe, T. Ueta, V. Peris, M. A. Groenewegen, J. A. Blommaert, M. Cohen, W. De Meester, G. J. Ferland, W. K. Gear, H. L. Gomez, P. C. Hargrave, E. Huygen, R. J. Ivison, C. Jean, S. J. Leeks, T. L. Lim, G. Olofsson, E. T. Polehampton, S. Regibo, P. Royer, B. M. Swinyard, B. Vandenbussche, H. Van Winckel, C. Waelkens, H. J. Walker, and R. Wesson. Herschel images of NGC 6720: H2 formation on dust grains. *Astronomy and Astrophysics*, 518(4):1–7, 2010.

[41] J. Vos, R. H. Østensen, P. Németh, E. M. Green, U. Heber, and H. Van Winckel. The orbits of subdwarf-B + main-sequence binaries: II. Three eccentric systems; BD+29°3070, BD+34°1543 and Feige 87. *Astronomy and Astrophysics*, 559, 2013.

[42] G. A. Walker, D. A. Bohlender, J. P. Maier, and E. K. Campbell. Identification of more interstellar C60+bands. *Astrophysical Journal Letters*, 812(1):L8, 2015.

[43] R. F. Webbink. Double white dwarfs as progenitors of R Coronae Borealis stars and Type I supernovae. *The Astrophysical Journal*, 1984.

[44] J. Woodall, M. Agúndez, A. J. Markwick-Kemper, and T. J. Millar. The UMIST database for astrochemistry 2006. *Astronomy and Astrophysics*, 466(3):1197–1204, 2007.

13 Kurzzusammenfassung

Heiße Unterzwerge befinden sich in deen letzten Phasen der Sternentwicklung. Wenn das Wasserstoffbrennen im Kern beendet ist entwickeln sich die Sterne über verschiedene mögliche Szenarien hin zu Objekten, die im Kern Helium brennen und nur eine dünne Atmosphäre besitzen.

Es gibt nicht viele bestätigte heiße Unterzwerge. Ihre Entstehung und die Eigenschaften der Population von heißen Unterzwergen sind noch nicht gut erforscht. Ein wichtiger Bestandteil für das Verständnis über heiße Unterzwerge liefern ihr photometrischen Eigenschaften. Diese werden allerdings durch das interstellare Medium, welches aus Gas und Staub besteht und für die Rötung und Extinktion des Lichtes verantwortlich ist, verändert. Diese Arbeit versucht diese Effekte zu berücksichtigen und sie zu korrigieren.

Für die Berechnung der extinktions- und rötungskorrigierten Werte der absoluten Magnitude und des Farbindexes für heiße Unterzwerge Kandidaten in den Grenzen der Staubkarte, habe ich eine Staubkarte und Gaia und APASS Daten genutzt. Außerdem habe ich die Unterscheide in der Benutzung von Gaia oder APASS Magnituden untersucht.

Bei allen drei Methoden (Gaia Magnituden und Entfernungen, Gaia Magnituden und 5 pc pro Würfel, APASS Magnituden und Gaia Entfernungen) zeigt die Rötungskorrektur, dass sie nicht für alle Sterne funktioniert, weil einige Sterne nach der Korrektur eine zu blaue Farbe besitzen. Die Anzahl der Sterne, bei denen die Korrektur nicht funktioniert, variiert stark von Methode zu Methode. Der Rest der Sterne erfüllt alle weiteren Kriterien bei der Benutzung von Gaia Magnituden. Bei der Benutzung von APASS Magnituden ist dies nicht der Fall.

Aufgrund von Selektionseffekten sind die Sterne auf unerwarteter Weise am Himmel verteilt.Gleiches gilt für die Extinktion. Daraus ergeben sich unerwartete Ergebnisse, wenn man die Entfernung und Position der Sterne, die die Kriterien für heiße Unterzwerge nicht erfüllen, am Himmel betrachtet.

Die Ergebnisse unterscheiden sich je nach Verwendung von Gaia oder APASS Magnituden. Dies hat eine Auswirkung darauf welche Sterne die Kriterien nicht erfüllen und ihre Eigenschaften nach der Korrektur. Ebenfalls der Anteil an ausgeschlossenen Sternen zeigt teilweise Unterscheide je nach Methode.

14 Appendix

14.1 Example data

l	b	G	M_G	$BP - RP$	M_V	$B - V$	A_V	$E(B-V)$	M_{Vcorr}	$(B-V)_{corr}$
103.521	-49.955	13.606	4.645	-0.319	4.633	-0.086	0.745	0.24	3.888	-0.326
48.05	-78.606	13.27	4.057	-0.429	4.069	-0.181	0.365	0.118	3.705	-0.299
74.559	-74.51	12.602	2.694	-0.199	2.711	-0.077	0.295	0.095	2.417	-0.172
110.263	-33.89	13.326	4.603	-0.361	4.592	-0.184	0.72	0.232	3.872	-0.416
108.729	-43.546	14.366	5.029	-0.493	5.089	-0.25	1.841	0.594	3.247	-0.844
106.843	-49.245	14.616	4.99	-0.298	5.011	-0.124	0.563	0.182	4.448	-0.306
36.239	-80.726	12.808	3.91	-0.219	3.966	-0.088	0.244	0.079	3.721	-0.167
102.968	-58.386	16.087	5.514	-0.428	5.505	-0.123	3.569	1.151	1.937	-1.274
103.361	-59.343	16.48	5.745	0.176	5.987	0.046	2.977	0.96	3.01	-0.914
113.166	-33.552	12.649	4.926	-0.384	4.882	-0.127	0.581	0.187	4.301	-0.314
105.999	-60.769	14.874	3.691	-0.33	3.718	-0.191	2.271	0.733	1.446	-0.924
117.157	-20.032	10.305	3.789	0.013	3.842	0.297	0.181	0.058	3.661	0.239
107.591	-62.532	15.553	4.249	-0.44	4.24	-0.097	2.121	0.684	2.119	-0.781
117.575	-19.8	12.419	4.573	0.16	4.685	0.083	0.183	0.059	4.502	0.024
112.142	-53.362	15.602	4.323	-0.357	4.317	-0.044	1.402	0.452	2.916	-0.496
78.29	-81.526	13.918	4.434	-0.443	4.48	-0.22	0.307	0.099	4.172	-0.319
112.565	-57.483	14.976	4.538	-0.501	4.503	-0.153	1.524	0.491	2.979	-0.644
116.07	-48.987	15.547	5.934	-0.399	6.027	-0.24	0.826	0.266	5.201	-0.506
119.241	-52.153	15.136	4.711	-0.396	4.716	-0.114	0.822	0.265	3.894	-0.379
311.579	-78.859	10.425	4.208	-0.32	4.242	-0.122	0.026	0.008	4.216	-0.13
118.863	-74.709	11.811	3.263	-0.648	3.21	-0.243	0.545	0.176	2.665	-0.419
121.32	-52.877	10.26	3.916	-0.377	3.928	-0.203	0.377	0.121	3.551	-0.324
121.251	-59.231	12.363	3.397	0.215	3.357	0.201	1.237	0.399	2.12	-0.198
122.308	-72.3	14.47	4.673	-0.556	4.686	-0.206	0.746	0.241	3.94	-0.447
122.849	-72.795	14.258	3.418	0.189	3.455	0.136	0.801	0.258	2.654	-0.122
122.937	-53.513	14.201	4.078	0.23	4.152	0.146	0.817	0.264	3.335	-0.118
123.96	-43.677	6.198	1.771	-1.839	1.499	0.84	0.007	0.002	1.492	0.838
123.526	-2.627	10.172	6.068	0.34	6.107	0.171	0.015	0.005	6.093	0.166
126.518	-60.913	15.126	4.968	-0.508	4.942	-0.157	1.194	0.385	3.748	-0.542
125.939	-47.085	12.062	4.598	-0.469	4.592	-0.152	1.47	0.474	3.122	-0.626
129.105	-58.49	12.047	4.168	-0.425	4.129	-0.158	0.941	0.303	3.188	-0.461

Table 2: Example data of stars in the selection

14.2 Python program

```python
In [1]: import h5py                                      #to read HDF5 files
        from itertools import islice                     #to slice lists into sublists
        import math
        import numpy as np
        import pandas as pd
        from astropy.coordinates import SkyCoord         #for coordinate transformations
        from astropy import units as u
        import matplotlib.lines as mlines
        import matplotlib.pyplot as plt
        import astropy.coordinates as coord

In [2]: df=pd.read_csv('full_sample_magnitudes_with_cartesian.csv',sep=';',header=0)
        Plx = df['Plx'].values.tolist()                  #convert all needed coloumns of
        ePlx = df['e_Plx'].values.tolist()               #the file into lists
        no = df['no'].values.tolist()
        rg=df['RAJ2000'].values.tolist()
        rd=df['DEJ2000'].values.tolist()
        dis=df['dis'].values.tolist()
        x = df['x'].values.tolist()
        y = df['y'].values.tolist()
        z = df['z'].values.tolist()
        BPRP = df['BP-RP'].values.tolist()
        Gmag = df['Gmag'].values.tolist()
        eGmag = df['e_Gmag'].values.tolist()
        BMag = df['BAPASS'].values.tolist()
        VMag = df['VAPASS'].values.tolist()

        Bmag = []
        Vmag = []
        for f in range(0, len(BMag)):
            try:                                         #determine which stars have B APASS data
                if float(BMag[f])>0:
                    Bmag.append((BMag[f], f))
            except ValueError:
                pass

        for e in range(0, len(VMag)):
            try:                                         #determine which stars have V APASS data
                if float(VMag[e])>0:
                    Vmag.append((VMag[e], e))
            except ValueError:
                pass

        apassmag = []
        for a in range(0, len(Vmag)):                    #get those stars which have both B and V data
            for b in range(0, len(Bmag)):
                if Vmag[a][1]==Bmag[b][1]:
                    apassmag.append((Vmag[a][0], Bmag[b][0], Vmag[a][1]))

        no0 = []
        apassno0 = []
        for g in range(0, len(apassmag)):
```

```
              if float(apassmag[g][0])>0:        #to get the row numbers
                  no0.append(apassmag[g][2])
                  apassno0.append(g)

          no_1 = []
          apassno_1 = []
          for h in range(0, len(no0)):
              if np.sign(Plx[h])==1.0:          #kick out the stars with negative parallax
                  no_1.append(no0[h])
                  apassno_1.append(apassno0[h])

          no1=[]
          apassno1 = []
          for i in range(0, len(no_1)):
              if 5*ePlx[no_1[i]]<Plx[no_1[i]]:      #kick outstars with error>20%
                  no1.append(no_1[i])
                  apassno1.append(apassno_1[i])

In [3]: z_min = -297.5                            #Check if star is within z direction bounds,
        z_max = -292.5                            #if so save all coords of the star
        no2=[]
        apassno2 = []
        for j in range(0,len(no1)):
            for i in range(0,119):
                if z_min+5*i <= z[no1[j]] <= z_max+5*i:
                    no2.append(no1[j])
                    apassno2.append(apassno1[j])

In [4]: x_min = -1997.5                           #Check if star is within x direction bounds,
        x_max = -1992.5                           #if so save all coords of the star
        no3=[]
        apassno3 = []
        for k in range(0, len(no2)):
            for l in range(0, 799):
                if x_min+5*l <= x[no2[k]] <= x_max+5*l:
                    no3.append(no2[k])
                    apassno3.append(apassno2[k])

In [5]: y_min = -1997.5                           #Check if star is within y direction bounds,
        y_max = -1992.5                           #if so save all coords of the star
        no4=[]
        apassno4 = []
        for m in range(0, len(no3)):
            for n in range(0, 799):
                if y_min+5*n <= y[no3[m]] <= y_max+5*n:
                    no4.append(no3[m])
                    apassno4.append(apassno3[m])

In [6]: def LinePlaneCollision(planeNormal, planePoint, rayDirection, rayPoint, epsilon=1e-6):
            """this funcion calculates the intersection point of a line and a plane"""

            ndotu = planeNormal.dot(rayDirection)
            if abs(ndotu) < epsilon:
                raise RuntimeError("no intersection or line is within plane")
```

```
            w = rayPoint - planePoint
            si = -planeNormal.dot(w) / ndotu
            Psi = w + si * rayDirection + planePoint
            return Psi
```

```
In [7]: A=[]
        B=[]
        C=[]
        InterA=[]
        InterB=[]
        InterC=[]
        OutputAcorr=[]
        OutputBcorr=[]
        OutputCcorr=[]
        for k in range(0,len(no4)):
            a = math.floor(abs((abs(x[no4[k]])-2.5)/5)) #How many planes are needed for each star?
            b = math.floor(abs((abs(y[no4[k]])-2.5)/5))
            c = math.floor(abs((abs(z[no4[k]])-2.5)/5))
            A.append(a+1)
            B.append(b+1)
            C.append(c+1)
            if abs(x[no4[k]])<2.5:
                InterA.append([0, 0, 0])
            else:
                for l in range(0,A[k]):
                    intera = LinePlaneCollision(planeNormal=np.array([1,0,0]),
                                                planePoint=np.array([2.5+l*5,0,0]),
                                                rayDirection=np.array([x[no4[k]],y[no4[k]],z[no4[k]]]),
                                                rayPoint=np.array([0,0,0]))
                    InterA.append(intera)          #Calculates the intersection points for x direction
            if abs(y[no4[k]])<2.5:                 #everything is calculated in the positive of each
                InterB.append([0, 0, 0])           #direction which gives no wrong values except for
            else:                                  #the sign since the problem is pointsymmetric in
                for m in range(0,B[k]):            #respect to the origin and this error is corrected lat
                    interb = LinePlaneCollision(planeNormal=np.array([0,1,0]),
                                                planePoint=np.array([0,2.5+m*5,0]),
                                                rayDirection=np.array([x[no4[k]],y[no4[k]],z[no4[k]]]),
                                                rayPoint=np.array([0,0,0]))
                    InterB.append(interb)
            if abs(z[no4[k]])<2.5:
                InterC.append([0, 0, 0])
            else:
                for n in range(0,C[k]):
                    interc = LinePlaneCollision(planeNormal=np.array([0,0,1]),
                                                planePoint=np.array([0,0,2.5+n*5]),
                                                rayDirection=np.array([x[no4[k]],y[no4[k]],z[no4[k]]]),
                                                rayPoint=np.array([0,0,0]))
                    InterC.append(interc)
```

```
In [8]: InputA = iter(InterA)
        OutputA = [np.vstack(list(islice(InputA, abs(elem))))
                    for elem in A]                              #Split the list into an array for each star
        for k in range(0,len(no4)):
```

```python
             if np.sign(x[no4[k]])==-1.0:
                 negA = np.negative(OutputA[k])          #Check if a star has negative coords,
                 OutputAcorr.append(negA)                #if so change the sign
             else:
                 OutputAcorr.append(OutputA[k])          #If not do nothing to coords

         InputB = iter(InterB)
         OutputB = [np.vstack(list(islice(InputB, abs(elem))))
                     for elem in B]
         for k in range(0,len(no4)):
             if np.sign(y[no4[k]])==-1.0:
                 negB = np.negative(OutputB[k])
                 OutputBcorr.append(negB)
             else:
                 OutputBcorr.append(OutputB[k])

         InputC = iter(InterC)
         OutputC = [np.vstack(list(islice(InputC, abs(elem))))
                     for elem in C]
         for k in range(0,len(no4)):
             if np.sign(z[no4[k]])==-1.0:
                 negC = np.negative(OutputC[k])
                 OutputCcorr.append(negC)
             else:
                 OutputCcorr.append(OutputC[k])

In [9]: Star=[]
        for k in range(0,len(no4)):     #put the coordinates of the different axis together
            star = [OutputAcorr[k], OutputBcorr[k], OutputCcorr[k]]
            Star.append(star)            #each direction still has it's own array

In [10]: Stars=[]
         for k in range(0,len(no4)):      #make one array per star with the coords
             stars = np.vstack([Star[k][0], Star[k][1], Star[k][2]])
             Stars.append(stars)

In [11]: def sortfirst(val):
             """returs the absolute value of the input.
             This is for sorting the coords in respect to x axis"""
             return abs(val[0])

In [12]: Starslist=[]
         for k in range(0,len(no4)):
             starlist = Stars[k].tolist()        #makes a list from the arrays
             Starslist.append(starlist)

In [13]: Starslistsorted=[]
         for k in range(0,len(no4)):                #sorts the coords based on x axis value
             starlistsorted = sorted(Starslist[k], key=sortfirst)
             Starslistsorted.append(starlistsorted)

In [14]: cubesthrough=[]                            #gives the cubes through which the light travels
         for k in range(0,len(no4)):
             gridstart=[399, 399, 59]
```

40

```python
        cubesthrough.append([gridstart[0], gridstart[1], gridstart[2]])
        for m in range(0,len(Starslistsorted[k])):              #do it for each star
            for n in range(0, len(OutputAcorr[k])):              #in x direction
                if math.isclose(abs(Starslistsorted[k][m][0]),
                                2.5+5*n, abs_tol=1e-06) is True:
                    #because the plane intersections don't necessarily give exact numbers
                    #but numbers with an error of about 1e-10 this step is needed
                    if np.sign(Starslistsorted[k][m][0])==-1.0:
                        gridstart[0] = gridstart[0]-1   #for negative x direction substract from cube
                    else:
                        gridstart[0] = gridstart[0]+1   #for positive direction add to cube number
                    cubesthrough.append([gridstart[0], gridstart[1], gridstart[2]])
            for p in range(0, len(OutputBcorr[k])):       #in y direction
                if math.isclose(abs(Starslistsorted[k][m][1]),
                                2.5+5*p, abs_tol=1e-06) is True:
                    if np.sign(Starslistsorted[k][m][1])==-1.0:
                        gridstart[1] = gridstart[1]-1
                    else:
                        gridstart[1] = gridstart[1]+1
                    cubesthrough.append([gridstart[0], gridstart[1], gridstart[2]])
            for q in range(0, len(OutputCcorr[k])):      #in z direction
                if math.isclose(abs(Starslistsorted[k][m][2]),
                                2.5+5*q, abs_tol=1e-06) is True:
                    if np.sign(Starslistsorted[k][m][2])==-1.0:
                        gridstart[2] = gridstart[2]-1
                    else:
                        gridstart[2] = gridstart[2]+1
                    cubesthrough.append([gridstart[0], gridstart[1], gridstart[2]])
```

In [15]:
```python
length=[]
for k in range(0,len(no4)):     #makes a list of all the numbers of intersections of each star
    if [0.0, 0.0, 0.0] in Starslistsorted[k]:
        length.append(len(Starslistsorted[k]))
    else:
        length.append(len(Starslistsorted[k])+1)
```

In [16]:
```python
Icubesthrough = iter(cubesthrough)       #makes a single sublist for each star
cubesthroughstar = [np.vstack(list(islice(Icubesthrough, elem)))
                        for elem in length]
```

In [17]:
```python
for r in range(0, len(no4)):     #adds the origin to those sublists which not yet have it in them
    if [0.0, 0.0, 0.0] not in Starslistsorted[r]:
        Starslistsorted[r].insert(0, [0.0, 0.0, 0.0])
    Starslistsorted[r].append([x[no4[r]], y[no4[r]], z[no4[r]]])
```

In [18]:
```python
Diff=[]
for s in range(0, len(no4)):     #calculates the distance travelled through each cube
    for t in range(0, len(Starslistsorted[s])-1):
        xdiff = Starslistsorted[s][t+1][0]-Starslistsorted[s][t][0]
        ydiff = Starslistsorted[s][t+1][1]-Starslistsorted[s][t][1]
        zdiff = Starslistsorted[s][t+1][2]-Starslistsorted[s][t][2]
        path = math.sqrt(xdiff**2+ydiff**2+zdiff**2)
        Diff.append(path)
```

```
In [19]: IDiff = iter(Diff)
         Diffstar = [np.vstack(list(islice(IDiff, elem)))
                         for elem in length]        #makes a sublist for each star

In [20]: with h5py.File("stilism_cube.h5", "r") as cube:
             data1 = cube.get("stilism/cube_err_magnitudemin")
             cubelowermagerr = np.array(data1)
         #turns the dataset into a numpy array to work with
         with h5py.File("stilism_cube.h5", "r") as cube:
             data3 = cube.get("stilism/cube_err_magnitudemax")
             cubeuppermagerr = np.array(data3)

In [21]: redstarlowermagerr = []
         redstaruppermagerr = []
         for h in range(0, len(no4)):
             redstarlowermagerr.append(cubelowermagerr[cubesthroughstar[h][-1][0]]
                             [cubesthroughstar[h][-1][1]][cubesthroughstar[h][-1][2]])
             redstaruppermagerr.append(cubeuppermagerr[cubesthroughstar[h][-1][0]]
                             [cubesthroughstar[h][-1][1]][cubesthroughstar[h][-1][2]])

In [22]: with h5py.File("stilism_cube.h5", "r") as cube:
             data1 = cube.get("stilism/cube_datas")
             cubedatas = np.array(data1)

In [23]: redcube=[]
         for v in range(0,len(no4)):      #calculates the absolute reddening per cube
             for w in range(0, length[v]):
                 red = Diffstar[v][w]*cubedatas[cubesthroughstar[v][w][0]]\
                         [cubesthroughstar[v][w][1]][cubesthroughstar[v][w][2]]
                 redcube.append(red)

In [24]: Iredcube = iter(redcube)
         redcubestar = [np.vstack(list(islice(Iredcube, elem)))
                         for elem in length]        #makes a sublist for each star

In [25]: redstar=[]
         for a in range(0, len(no4)):
             redsum = sum(redcubestar[a])     #calculates the absolute reddening per star
             extsum = 3.1*sum(redcubestar[a])
             redstar.append(redsum)

In [26]: Absmag=[]
         Absmagerrmax=[]
         Absmagerrmin=[]
         for b in range(0,len(no4)):        #calculates the absolute magnitude
             absmag = Gmag[no4[b]]-3.1*redstar[b]\
                     +5*(np.log10(Plx[no4[b]]/1000)+1)
             absmagu = Gmag[no4[b]]+5*(np.log10(Plx[no4[b]]/1000)+1)
             absmagerrmax = redstaruppermagerr[b]\
                         +(5/(ePlx[no4[b]]*np.log(10)))*Plx[no4[b]]+eGmag[no4[b]]
             absmagerrmin = redstarlowermagerr[b]\
                         +(5/(ePlx[no4[b]]*np.log(10)))*Plx[no4[b]]+eGmag[no4[b]]
             Absmag.append((absmag, b, absmagu))
             Absmagerrmax.append(absmagerrmax)
             Absmagerrmin.append(absmagerrmin)
```

42

```
In [27]: cecorr=[]
         for c in range(0, len(no4)):
             ce = BPRP[no4[c]]-redstar[c]     #calculates the corrected BP-RP
             cecorr.append(ce)

In [28]: Absmagce=[]
         no5=[]
         out=[]
         ceout=[]
         for d in range(0, len(no4)):                    #filters out too blue objects
             if cecorr[d]>-0.7:
                 Absmagce.append(Absmag[d])
                 no5.append(no4[d])
             else:
                 out.append((no4[d], Absmag[d][1]))
                 ceout.append(cecorr[d])

In [29]: Absmagran=[]
         for c in range(0,len(no5)):
             if -1.0<Absmagce[c][0]<7.0:          #checks the absolute magnitude criterion
                 Absmagran.append(Absmagce[c])
             else:
                 out.append((no5[c], Absmagce[c][1]))
                 ceout.append(cecorr[Absmagce[c][1]])

In [30]: bright=[]
         notbright=[]
         cenotbright=[]
         nonotbright=[]
         middle=[]
         dim=[]
         nobright=[]
         cebright=[]
         nomiddle=[]
         cemiddle=[]
         nodim=[]
         cedim=[]
         for d in range(0, len(Absmagran)): #sorts the stars in to bright, middle and dim
             if Absmagran[d][0]<1.0:
                 bright.append(Absmagran[d])
                 nobright.append(no4[d])
                 cebright.append(cecorr[Absmagran[d][1]])
             else:
                 notbright.append(Absmagran[d])
                 nonotbright.append(no4[d])
                 cenotbright.append(cecorr[Absmagran[d][1]])
         for i in range(0,len(notbright)):
             if 1.0<notbright[i][0]<3.8:
                 middle.append(notbright[i])
                 nomiddle.append(nonotbright[i])
                 cemiddle.append(cenotbright[i])
             else:
                 dim.append(notbright[i])
```

```
            nodim.append(nonotbright[i])
            cedim.append(cenotbright[i])

In [31]: Starswekeep=[]
         noswekeep=[]
         noswekeepb=[]
         noswekeepm=[]
         noswekeepd=[]
         outb=[]
         outm=[]
         outd=[]
         cein=[]
         for e in range(0, len(bright)):      #checks the additional criterion for bright stars
             if bright[e][0]>=11.76*cebright[e]+2.53:
                 Starswekeep.append(bright[e])
                 noswekeepb.append(nobright[e])
                 cein.append(cebright[e])
             else:
                 out.append((nobright[e], bright[e][1]))
                 outb.append((nobright[e], bright[e][1]))
                 ceout.append(cebright[e])
         for f in range(0,len(middle)):       #checks the additional criterion for middle stars
             if middle[f][0]>=5.6*cemiddle[f]+1.84:
                 Starswekeep.append(middle[f])
                 noswekeepm.append(nomiddle[f])
                 cein.append(cemiddle[f])
             else:
                 out.append((nomiddle[f], middle[f][1]))
                 outm.append((nomiddle[f], middle[f][1]))
                 ceout.append(cemiddle[f])
         for g in range(0, len(dim)):         #checks the additional criterion for dim stars
             if dim[g][0]>=16*cedim[g]-1.8:
                 Starswekeep.append(dim[g])
                 noswekeepd.append(nodim[g])
                 cein.append(cedim[g])
             else:
                 out.append((nodim[g], dim[g][1]))
                 outd.append((nodim[g], dim[g][1]))
                 ceout.append(cedim[g])
```

Statutory Decleration

I herewith declare that I have composed the present thesis myself and without use of any other than the cited sources and aids. Sentences or parts of sentences quoted literally are marked as such; other references with regard to the statement and scope are indicated by full details of the publications concerned. The thesis in the same or similar form has notbeen submitted to any examination body and has not been published.This thesis was not yet, even in part, used in another examination or as a course performance.

Declaration of Consent

We inform you that, when submitting your work (term paper/ bachelorthesis/ masterthesis), plagiarism detection software will beused to ensure that your workwas writtenaccording to the guidelinesof scientific work.With your signature you acknowledge this and agree to it.

_____   _____
Place, Date   Signature